© 2020. Published by The Company of Biologists Ltd | Development (2020) 147, dev185579. doi:10.1242/dev.185579

PRIMER

Fluid flow as a driver of embryonic morphogenesis

Margo Daems*, Hanna M. Peacock* and Elizabeth A. V. Jones‡

ABSTRACT

Fluid flow is a powerful morphogenic force during embryonic development. The physical forces created by flowing fluids can either create morphogen gradients or be translated by mechanosensitive cells into biological changes in gene expression. In this Primer, we describe how fluid flow is created in different systems and highlight the important mechanosensitive signalling pathways involved for sensing and transducing flow during embryogenesis. Specifically, we describe how fluid flow helps establish left-right asymmetry in the early embryo and discuss the role of flow of blood, lymph and cerebrospinal fluid in sculpting the embryonic cardiovascular and nervous system.

KEY WORDS: Shear stress, Blood, Lymph, Cerebrospinal fluid, Cilia, Mechanosensation

Introduction

Much effort has been made to understand how fluid flow and its accompanying physical forces affect embryonic development. The activation of the right molecular pathway at the right time and place drives correct embryonic development, a process partly dependent on fluid flow. Fluid flow can create a morphogen gradient, driving important morphogenic changes during embryonic development. On the other hand, the physical forces created by fluid flow can be translated into a biological response by mechanosensitive cell types, which activates mechanosensitive pathways (summarised in Box 1 and Tables 1 and 2).

Even one century ago, it was clear that fluid flow affects embryonic development. The first such publication regarded the role of flow in cardiovascular development, where it was shown that removing the heart from a chick embryo impaired normal vascular development (Chapman, 1918). However, until the advent of modern imaging techniques and genetics (Table 3), these findings were largely observational. By now it is clear that fluid flow is not limited to cardiovascular development, but affects every organ system that is filled with fluids at some point in development. Recent work has shed further light on the contributions of fluid flow to embryonic development, at the tissue, cellular and molecular level. In this Primer, we describe the importance of fluid flow during early, cardiovascular and neurological embryonic development, while highlighting the mechanosensitive signalling pathways involved.

The physics of flow

Fluid flow is either laminar or turbulent (Fig. 1A). In laminar flow, adjacent layers of fluid (lamina) slide along one another without mixing. Each concentric layer reduces the friction on the wall for the next most inner layer, creating a parabolic flow profile. Laminar flow can be classified as steady, pulsatile or oscillatory (Fig. 1B). In steady flow patterns, there is a constant unidirectional flow present. In pulsatile flow patterns, the velocity of the laminar flow changes over time but remains unidirectional, whereas in oscillatory flow, backwards flow can also be observed. Turbulent flow is characterised as being irregular, with a chaotic mixing among the layers, which blunts the flow profile. Both oscillatory flow and turbulent flow are considered forms of disturbed flow.

Fluid flow creates a frictional force against the wall of the lumen, known as wall shear stress. In this case, 'stress' refers to physics terms for a force per unit area, and not a biological 'stress', such as that created by reactive oxygen species. Shear stress depends on the shear rate and the viscosity of the fluid. The rate of change of velocity defines the shear rate, with flow closer to the wall being slower than flow further away. Viscosity is the resistance of the flowing fluid; whole blood is more viscous than plasma, and thus shear stresses are greater for whole blood than for plasma.

Left-right asymmetry during early development

Perhaps the earliest influences of fluid flow can be observed in the establishment of left-right asymmetry shortly after gastrulation, although how fluid flow controls symmetry breaking is still highly debated. Left-right asymmetry is necessary for the development of mature organ shapes and the proper positioning of the organs (Blum and Ott, 2018). Left-right asymmetry has been extensively studied in chick embryos, where it is characterised by distinct gene expression patterns on each side of the embryo, with *Nodal*, *Lefty* and *Pitx2* expression on the left side of the lateral plate mesoderm, and *Cerberus* expression on the right (Fig. 2A) (Levin et al., 1995; Logan et al., 1998). In particular, left-sided expression of *Pitx2* is crucial for left-right patterning, as alterations of *Pitx2* expression in chick and *Xenopus* embryos affect the direction of body rotation, and $Pitx2^{-/-}$ mouse embryos present with laterality defects (Ryan et al., 1998).

Breaking of lateral symmetry is suspected to be initiated by cilia-driven fluid flow in the vertebrate embryo. Motile cilia are located in the left-right organiser (LRO) of the embryo. For mouse embryos, this is located on the ventral surface of the node; for zebrafish, on the inner surface of Kupffer's vesicle (Nonaka et al., 1998, 2002; Okabe et al., 2008; Okada et al., 2005). In mouse and *Xenopus* embryos, motile cilia are positioned at the posterior side of the LRO cells by the planar cell polarity (PCP) pathway, creating a posterior tilt of the cilium (Nonaka et al., 2005). In mouse embryos, this process is additionally driven by posterior *Wnt5a*/*b* expression patterns, as polarisation of the node cells is impaired in $Wnt5a^{-/-}$ and $Wnt5b^{-/-}$ embryos (Minegishi et al., 2017). The created posterior tilt is crucial for generating an effective leftward ciliary stroke, resulting in a right-to-left flow of the extracellular fluids (Nonaka et al., 2005). Computational analysis of cilia-driven flow has shown that, without this tilt, vertical cilia would create small recirculating flows around each cilia, rather than a directional flow across the whole node

Department of Cardiovascular Sciences, Centre for Molecular and Vascular Biology, KU Leuven, 3000 Leuven, Belgium.
*These authors contributed equally to this work

‡Author for correspondence (liz.jones@kuleuven.be)

M.D., 0000-0002-6961-644X; H.M.P., 0000-0002-2530-6271; E.A.V.J., 0000-0002-2006-7064

Development (2020) 147, dev185579. doi:10.1242/dev.185579

Box 1. Overview of proposed mechanosensors and mechanosensory pathways

Molecular mechanosensors are of crucial importance during embryonic development. Physical forces, such as shear stress and cyclic stretch, directly act on these molecules, which either activates downstream mechanosensitive pathways or changes their expression level to create a complex and integrated biological response. Interestingly several mechanosensors are shared between organ systems, such as the Ca^{2+} channel Trpp2, which is important for left-right patterning as well as blood flow sensing.

Mechanosensors (Table 1) activate a number of mechanosensitive pathways (Table 2). Although endothelial mechanosensation has been studied extensively (Givens and Tzima, 2016), it remains unclear exactly how endothelial cells translate mechanical cues to a biological response. The concepts behind endothelial mechanotransduction are continuously evolving owing to its heterogeneity, although it is becoming clear that several mechanosensors and mechanosensitive pathways intensively interact with each other. No one system can fully explain mechanosensation; it is the combination of mechano-transduced signals originating from different pathways that defines the ultimate outcome of these physical forces in endothelial cells (Givens and Tzima, 2016).

(Cartwright et al., 2004). The overall distribution of cilia is also biased, with a higher density of cilia in the anterior region of Kupffer's vesicle, which creates a faster fluid flow (Ferreira et al., 2017; Wang et al., 2011a). The PCP pathway (driven by Wnt signalling) further specifies the posterior tilt of motile cilia through Vangl2 in zebrafish embryos (Borovina et al., 2010; Song et al., 2010). Indeed, cilia are dispersed randomly in *Vangl1/2*$^{-/-}$ zebrafish embryos and nodal flow is turbulent, resulting in disruption of left-right patterning (Borovina et al., 2010; Song et al., 2010).

There are two proposed mechanisms for how interstitial fluid flow initiates left-right patterning, either through mechanosensation (Fig. 2B) or by creating a morphogen gradient (Fig. 2C). A fraction of cilia are immotile and it has been suggested that the immotile cilia sense flow (McGrath et al., 2003; Sampaio et al., 2014). Crown cells in the node of mouse embryos and Kupffer's vesicle in zebrafish have immotile cilium equipped with mechanosensitive Ca^{2+} channels, such as transient receptor potential polycystin 2 (Trpp, previously known as polycystin 2 or Pkd2) (McGrath et al., 2003; Schottenfeld et al., 2007; Yoshiba et al., 2012) (Fig. 2B). The activation of Trpp2 induces Ca^{2+} oscillations in the cilium, resulting in leftward Nodal expression and the initiation of vertebrate left-right asymmetry (Yuan et al., 2015). In the zebrafish embryo, the increased cytoplasmic Ca^{2+} levels block *Cerberus* expression, so that *Nodal* is expressed on the left side of the zebrafish embryo (Piccolo et al., 1999). *Xenopus* embryos lacking *trpp2* fail to develop left-side oriented *Nodal* expression (Vick et al., 2018). However, it remains unclear how the primary cilium senses the nodal flow because, in mouse and *Xenopus* embryos, for example, the direction of nodal flow defines left-right patterning. It has therefore been hypothesised that primary cilia either detect an asymmetric flow velocity (Sampaio et al., 2014) or detect the specific direction of the flow (McGrath et al., 2003), or that motile cilia sense their own movement by amplifying the asymmetry of the LRO (Cartwright et al., 2020; Ferreira et al., 2018, 2019). But it remains unclear whether primary cilia can sense the low flow present in the LRO or whether they can distinguish the direction of flow (Cartwright et al., 2020; Ferreira et al., 2019).

As mentioned, rather than sensing flow, a chemo-sensory mechanism of left-right patterning has also been proposed. Here, cilia-driven fluid flow distributes nodal vesicular particles containing retinoic acid and sonic hedgehog towards the left side of the embryo, creating a morphogen gradient (Ferreira et al., 2017; Okada et al., 2005; Tanaka et al., 2005) (Fig. 2C). However, mathematical models suggest that nodal flow rates are insufficient to transport large vesicles and are simply too strong to create a gradient of small proteins, instead creating a symmetric distribution (Omori et al., 2018).

The presence and necessity of nodal flow remains unclear in some species, such as pig and chick embryos. In the chick embryo, cells of the Hensen's node rearrange themselves asymmetrically, creating a leftward movement of the cells around the node (Gros et al., 2009). The relative displacement establishes an asymmetric gene expression pattern of *Shh* and *Fgf8*, and initiates left-right patterning (Gros et al., 2009). Although differences occur, left-right patterning is well conserved between vertebrate species.

Blood flow

Although the initial specification of the cardiovascular system is determined by genetic cues, physical forces created by blood flow are crucial for its proper maturation as soon as the heart begins to beat (Jones et al., 2006). Mechanotransduction, the sensing of physical forces and their translation into a biological response, is an inherent function of endothelial cells (Jones, 2011). To enable proper mechanotransduction, endothelial cells are equipped with various mechanosensors that activate a number of signalling pathways (summarised in Box 1). During cardiovascular development, physical forces sensed by endothelial cells drive proper heart morphogenesis, vascular remodelling, arterial-venous specification, lymphatic valve formation and the development of haematopoietic stem cells (HSCs).

Heart and great vessel morphogenesis

In mice, the primary heart tube starts rhythmically contracting at E8.25, which initiates blood flow through the vasculature of the yolk sac and embryo proper (Nishii and Shibata, 2006). This blood flow is crucial for sculpting the heart and great vessels, the dorsal aortae and cardinal vein. As such, disrupting flow within the developing heart induces both cardiac and vascular malformations (Hove et al., 2003; Hu et al., 2009).

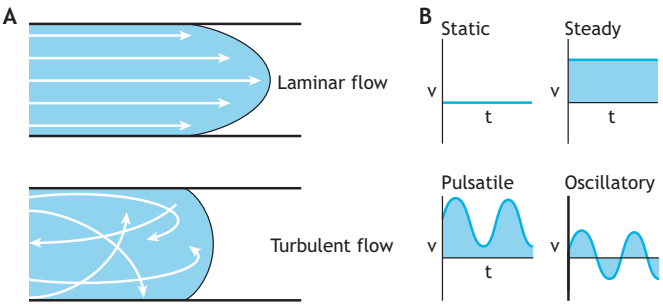

Fig. 1. The physics of flow. Schematic overview of laminar (top) and turbulent (bottom) flow patterns. In laminar flow, adjacent layers of fluid slide across one another, creating a parabolic flow profile. In turbulent flow, layers of fluid are mixed with one another, blunting the flow profile. (B) Laminar flow can be further divided into steady, pulsatile and oscillatory flow patterns. Static flow patterns resemble the absence of flow, while there is a constant laminar flow in steady flow patterns. In pulsatile flow patterns, the velocity of the laminar flow changes over time but remains unidirectional, while in oscillatory flow patterns, backwards flow can also be observed, illustrated by negative velocities on the diagram. t, time; v, velocity.

Development (2020) 147, dev185579. doi:10.1242/dev.185579

Table 1. Summary of known mechanosensors

Mechanosensor	Location of activity	Reference
Ion channels		
Kir2.1	Vascular system	Hoger et al. (2002); Olesen et al. (1988)
Trpv4	Vascular system	Goedicke-Fritz et al. (2015); Hartmannsgruber et al. (2007); Ma et al. (2010)
	Kidney cells	Pochynyuk et al. (2013)
	Osteocytes	Corrigan et al. (2018); Masuyama et al. (2008)
Polycystin 1 and polycystin 2	Vascular system	Aboualaiwi et al. (2009); Nauli et al. (2008)
	Lymphatic system	Outeda et al. (2014)
	Kidney cells	Nauli et al. (2003); Praetorius and Spring (2003)
	Left-right patterning	McGrath et al. (2003); Schottenfeld et al. (2007); Yoshiba et al. (2012)
	CSF-contacting neurons	Sternberg et al. (2018)
	Radial glial cells	Guirao et al. (2010); Mirzadeh et al. (2010); Ohata et al. (2015)
	Osteocytes	Xiao et al. (2011)
Piezo1 channel	Vascular system	Li et al. (2014a); Ranade et al. (2014)
	Lymphatic system	Nonomura et al. (2018)
	Osteocytes	Wang et al. (2020)
	Kidney cells	Peyronnet et al. (2013)
Junctional mechanosensory complex	Vascular system	Tzima et al. (2005)
Primary/immobile cilium	Vascular system	Hierck et al. (2008)
	Left-right organiser	McGrath et al. (2003); Schottenfeld et al. (2007); Yoshiba et al. (2012)
	Brain ventricle	Grimes et al. (2016)
	Kidney cells	Praetorius and Spring (2003)
	Osteocytes	Whitfield (2003); Yuan et al. (2015)
	Odontoblastic cells (tooth)	Whitfield (2003)
Glycocalyx	Vascular system	Florian et al. (2003); Henderson-Toth et al. (2012)
	Kidney cells	Liew et al. (2017)
Caveolae	Vascular system	Rizzo et al. (2003); Sinha et al. (2011)
	Lymphatic system	Yang et al. (2016)
	Osteocytes	Gortazar et al. (2013)
Integrins	Vascular system	Jalali et al. (2001); Tzima et al. (2001)
	Lymphatic system	Bazigou et al. (2009)
	Kidney cells	Teräväinen et al. (2013)
	Osteocytes	Thi et al. (2013)

The development of heart and the vessels are inherently linked, as exemplified by the development of the aortic arch (Fig. 3). Initially, six pharyngeal arches are present that experience the same flow pattern. During cardiac looping, the outflow tract of the primary heart tube shifts to the right and takes on a C-shape, introducing a more complex geometry through which blood flows (Taber, 2006) (Fig. 3A). As a consequence, the pharyngeal arch that experiences the highest flow grows in diameter, while the others regress. In the chick embryo, physical disruption of blood flow by ligation of the vitelline vein or left atrium disrupts aortic arch selection by altering blood flow patterns in the pharyngeal arches (Hu et al., 2009; Kowalski et al., 2012). In the mouse embryo, PITX2 drives the rotation of the outflow tract during heart looping; loss of PITX2 results in randomised heart looping and randomised laterality or even doubling of the aortic arch (Yashiro et al., 2007) (Fig. 3B).

Shear stress in the heart modulates gene expression of endocardial cells: the endothelial cells lining the inside of the heart. The embryonic heart initially grows by trabeculation: the formation of columns of muscular tissue within the ventricles (Wittig and Münsterberg, 2016). The endocardium communicates with the underlying myocardium (heart muscle tissue), such that if the endocardium is absent, trabeculation does not occur even though blood flow is normal (Peshkovsky et al., 2011). In zebrafish embryos, the primary cilium of endocardial cells facilitates shear stress-induced *klf2a* expression in the endocardium and subsequent *notch1b* expression (Samsa et al., 2015). In mouse embryos, mechanosensation by endocardial primary cilia induces myocardial compaction (Slough et al., 2008). The shear stress-driven *klf2a* expression of the endocardium is necessary for compaction of the trabeculae into denser heart tissue and for myocardial wall integrity (Dietrich et al., 2014; Rasouli et al., 2018). The absence of myocardial compaction and wall integrity in *klf2a* mutant zebrafish embryos can be rescued by specific overexpression of *klf2a* in the endocardium, demonstrating the tight communication between both (Dietrich et al., 2014; Rasouli et al., 2018). This endocardial-myocardial signalling cascade is also activated by altered haemodynamic forces created by cardiac injury in zebrafish (Gálvez-Santisteban et al., 2019). Haemodynamic activation of *notch1b* induces *erbb2* expression and activates BMP signalling, which in turn promotes cardiomyocyte reprogramming and heart regeneration (Gálvez-Santisteban et al., 2019).

Blood flow through the ventricle coordinates growth and maturation of the myocardial cells lining the ventricle. Indeed, weak atrium (*wea*) mutant zebrafish have reduced blood flow without loss of ventricular contraction, resulting in reduced myocardial cell size and myofibril content (Lin et al., 2012). Furthermore, the elongation and orientation of cardiomyocytes in the outer aortic curvature is driven by blood flow and partially facilitates heart looping (Auman et al., 2007). As flow-driven elongation is lost, *wea* mutants have reduced curvatures and more cuboidal cell morphology in the outer curvature of the aorta (Auman et al., 2007).

During cardiac valve formation, oscillatory flow is necessary for proper valve development. The zebrafish heart has two chambers with three sets of valves: the outflow tract (OFT), the atrioventricular canal (AVC) and the inflow tract (IFT) valve (Fig. 4). As the heart takes shape, endocardial cells converge into the AVC to contribute to the cardiac valves, a migration driven by oscillatory shear stress (OSS) (Boselli et al., 2017). High OSS levels in the AVC of zebrafish embryos open mechanosensitive Trpp2 and Trpv4 (transient receptor potential cation channel subfamily V

Development (2020) 147, dev185579. doi:10.1242/dev.185579

Table 2. Examples of pathways involved in mechanosensory signal transduction during development

Mechanosensitive pathway	Active in	Reference
Klf2 signalling	Vascular system	Dekker et al. (2002); Parmar et al. (2006)
	Lymphatic system	Choi et al. (2017)
	Kidney cells	Zhong et al. (2018)
	Osteocytes	Kim et al. (2019)
Notch signalling	Vascular system	Driessen et al. (2018); Fang et al. (2017); Mack et al. (2017)
	Lymphatic system	Choi et al. (2017); Ricard et al. (2012)
Alk1/endoglin and Alk5 signalling	Vascular system	Baeyens et al. (2016); Corti et al. (2011); Peacock et al. (2020); Zhou et al. (2012)
Prox1/Foxc2/Gata2 signalling	Lymphatic system	Kazenwadel et al. (2012); Lim et al. (2012); Sweet et al. (2015)
PI3K/Akt signalling	Vascular system	Hong et al. (2006); Yang et al. (2016)
	Lymphatic system	Yang et al. (2016)
Yap/Taz signalling	Vascular system	Chiang et al. (2017); Dupont et al. (2011); Nakajima et al. (2017); Kim et al. (2017)
	Lymphatic system	Sabine et al. (2012)
	Kidney cells	Szeto et al. (2016)
Wnt/β-catenin signalling	Vascular system	Gelfand et al. (2011); Li et al. (2014b)
	Lymphatic system	Cha et al. (2016, 2018)
	Kidney cells	Germino (2005)
	Osteocytes	Gortazar et al. (2013)
Tie/Ang signalling	Vascular system,	Tressel et al. (2007)
	Lymphatic system	Dellinger et al. (2008); Li et al. (2014b)
Coup-TFII signalling	Vascular system	Chen et al. (2012)
Trpp2l1	CSF	Sternberg et al. (2018)
Plexin D1	Vascular system	Mehta et al. (2020)

member 4) channels, which induce *klf2a* expression (Heckel et al., 2015; Vermot et al., 2009). Furthermore, Piezo1 Ca^{2+} channels in endocardial cells are involved in OFT valve development and also induce *klf2a* expression (Duchemin et al., 2019). Haemodynamic endocardial *klf2a* activation drives different processes during cardiac valve formation. In the AVC and OFT, endocardial *klf2a* expression drives *notch1b* expression and the subsequent deposition of fibronectin, which is necessary for the rearrangement of cardiac valve leaflet cells (Duchemin et al., 2019; Steed et al., 2016; Vermot et al., 2009) (Fig. 4A,B). Both in the OFT and AVC region, endocardial *klf2a* activation induces *wnt9b* expression, which stimulates the cell proliferation and subsequent condensation of the remodelling cardiac cushion in underlying mesenchymal cells (Goddard et al., 2017) (Fig. 4A,B). As the OFT is surrounded by smooth muscle progenitors, endocardial *klf2a* activation ensures Yap1 nuclearisation, although the necessity of Yap1 remains unknown (Duchemin et al., 2019) (Fig. 4B). Besides *klf2a*, OSS also induces *miR-21* expression in the AVC, which prevents *spry2* expression, an inhibitor of the MAPK signalling pathway. With *spry2* expression inhibited, MAPK signalling is active, driving the proliferation of valve-forming cells and inhibiting *notch1b* signalling (Banjo et al., 2013). As such, OSS both upregulates and inhibits *notch1b* expression depending on the pathway, possibly implying feedback loops that operate on different time scales.

Arteriovenous differentiation

Genetic cues initiate arterial and venous cell fate in endothelial cells that form the primitive vascular plexus. In early zebrafish vasculature, presumptive arterial endothelial cells express *efnb2*, *notch1b*, *notch3/5* and gridlock (*grl*), and the expression of venous marker *flt4* is already restricted to the posterior cardinal vein (Lawson et al., 2001; Zhong et al., 2000). In the early mammalian vasculature, Cx37 (*Gja4*), *Dll4* and *Hey1* are expressed in arteries before the onset of flow, whereas there are no genes specifically restricted to the venous vessels (Chong et al., 2011). However, the arterial-venous identity of endothelial cells is susceptible to modification by fluid flow. In chick embryos, transplanting arterial endothelial cells into a vein, or vice versa, adapts them to the new environment (Moyon et al., 2001). In zebrafish, the number of arterial and venous intersegmental vessels is pre-defined by heterogeneous Notch activation, but the balance between arterial and venous intersegmental vessels is fine-tuned by shear stress (Geudens et al., 2019). After connecting the intersegmental vessels to venous circulation, venous endothelial cells migrate against flow to replace arterial endothelial cells of the intersegmental vessel (Weijts et al., 2018). In presumptive arterial intersegmental vessels with higher flow, flow-induced Notch signalling prevents this venularisation (Weijts et al., 2018). Similarly, in mice, blood flow is necessary for arterial-specific *Notch1* expression (Jahnsen et al., 2015).

Vascular remodelling

A primitive vascular plexus forms at E7.0 in mice and consists of capillaries lacking mural cell support or an extensive basement membrane. The vasculature is subsequently remodelled to efficiently supply the growing embryo. Shortly after the first irregular primitive heart tube contractions, erythrocytes enter circulation and the subsequent increase in viscosity initiates vascular remodelling (Al-Roubaie et al., 2011; Lucitti et al., 2007; McGrath et al., 2003). When erythrocytes are blocked from entering circulation (e.g. by trapping them in the blood islands), shear stress levels do not increase and the yolk sac vasculature does not remodel (Lucitti et al., 2007). The same phenotype is observed when haematopoiesis is impaired and red blood cells do not differentiate in the blood islands (e.g. mutations in *Rapgef2* or *Myc*) (He et al., 2008; Satyanarayana et al., 2010). However, injecting a starch solution, which is viscous and therefore restores blood viscosity, rescues vascular remodelling, suggesting that it is shear stress that initiates vascular remodelling and not erythrocytes themselves (Lucitti et al., 2007).

Although shear stress is well acknowledged to drive remodelling, the role of mechanotransduction is less straightforward, as embryos still remodel surprisingly well even in the absence of certain mechanosensors or mechanosensitive pathways. Loss of *Klf2*, one of the principal transcription factors driving mechanotransduction, is embryonic lethal but only after initial remodelling has occurred

Development (2020) 147, dev185579. doi:10.1242/dev.185579

Table 3. Tools for studying flow *in vivo*

Model	System	Methods or details	Reference
Erythrocyte trap	Vascular	Trap erythrocytes in the blood islands using acrylamide/TEMED injection. This prevents the viscosity increase needed to start vascular remodelling.	Lucitti et al. (2007)
Ligation	Vascular	Ligate the vessels of interest, such as vitelline vein or pharyngeal arch arteries.	le Noble et al. (2003); Yashiro et al. (2007)
Concurrent time lapse imaging	Vascular CSF flow	Inject fluorescent beads in the major arteries, veins or brain ventricles; concurrently image fluorescent beads and vasculature or ventricles and central canal.	Karthik et al. (2018); Thouvenin et al. (2020)
Computational modelling of flow	Vascular CSF flow	Use computational fluid dynamics, based on imaged flow patterns, to calculate the shear stresses. Used in both embryo and retina models.	Bernabeu et al. (2014); Eichele et al. (2020); Thouvenin et al. (2020)
Genetic models			
Impaired haematopoiesis	Vascular	Impaired haematopoiesis results in reduced numbers of erythrocytes and prevents the necessary viscosity increase to start vascular remodelling; e.g. *Myc*$^{-/-}$, *RapGEF2*$^{-/-}$	He et al. (2008); Satyanarayana et al. (2010)
Mechanosensor	Vascular lymphatic cerebrospinal fluid	Impaired mechanosensation prevents mechanical cues from being translated into physical cues, e.g. in *Piezo1*$^{-/-}$, and *Trpp1* and *Trpp2* mutants.	Li et al. (2014a); Ohata et al. (2015)
Impaired heart beat	Vascular	*Ncx1*$^{-/-}$ mice lack a heartbeat and blood flow but survive until E10; *tnnt2*$^{-/-}$ zebrafish show reduced cardiac contractility and reduced blood flow. This allows the study of vascular remodelling in the absence of blood flow.	Koushik et al. (2001); Sehnert et al. (2002)
Motile cilia	Vascular CSF flow Left-right organiser	Genetic defects affecting ciliary motility or ciliogenesis, e.g. *Dnah5*$^{-/-}$, *Ift88*$^{-/-}$, *Ift57*$^{-/-}$, *Ift787*$^{-/-}$	Banizs et al. (2005); Ibañez-Tallon et al. (2004); Kramer-Zucker et al. (2005)

(Kuo et al., 1997). Similarly, endothelial-specific *Yap* ablation does not prevent remodelling between E8.5 and E9.5 but leads to later embryonic lethality (Zhang et al., 2014). Similarly, impairment of some mechanosensors results in remodelling defects but impairment of others does not. Endothelial-specific deletion of *Ift88* is non-lethal (Dinsmore and Reiter, 2016), whereas endothelial ablation of *Piezo1* does prevent remodelling, although differences in genetic background appear to allow survival of the embryo in the absence of the protein, likely due to differences in the stage at which the protein is first deleted (Li et al., 2014a; Nonomura et al., 2018). Overall, these conflicting results indicate that there is a lot of redundancy in mechanotransduction, such that deleting any individual pathway or mechanosensor cannot prevent remodelling as a whole.

Flow also influences vascular remodelling, which includes sprouting angiogenesis, intussusceptive angiogenesis, and regression and fusion of vessels (Fig. 5). During sprouting angiogenesis, VEGF gradients initiate vascular sprouts from existing vessels (Gerhardt et al., 2003). However, flow dynamics fine-tune the VEGF-driven sprouting process, with sprouts forming exclusively at shear stress minima (Ghaffari et al., 2015; Song and Munn, 2011) (Fig. 5A). How these shear stress minima are sensed is not known, but may involve cilia; primary cilia are equipped with Trpp2 Ca^{2+} channels and loss of *Trpp2* in zebrafish reduces the number of tip cells in the developing vasculature (Goetz et al., 2014). Although VEGF initiates sprouting, VEGF distribution is not simply defined by passive diffusion, but is determined by interstitial flow (Ghaffari et al., 2017). Increased interstitial flow in the direction of sprouting enhances sprouting and sprout extension follows the interstitial flow patterns (Akbari et al., 2019; Ghaffari et al., 2017; Kim et al., 2016). Furthermore, sprout elongation follows the interstitial flow patterns and the speed of elongation is proportional to the magnitude of interstitial flow (Ghaffari et al., 2017).

New vessels can also be formed by intussusceptive angiogenesis, when a vessel is split longitudinally. Here, endothelial cells form pillars that grow across the vessel lumen (Burri and Djonov, 2002). These pillars are invaded by fibroblasts and pericytes, until eventually the vessel splits (Burri and Djonov, 2002). High shear stress levels facilitate rapid pillar growth, although pillars fuse to

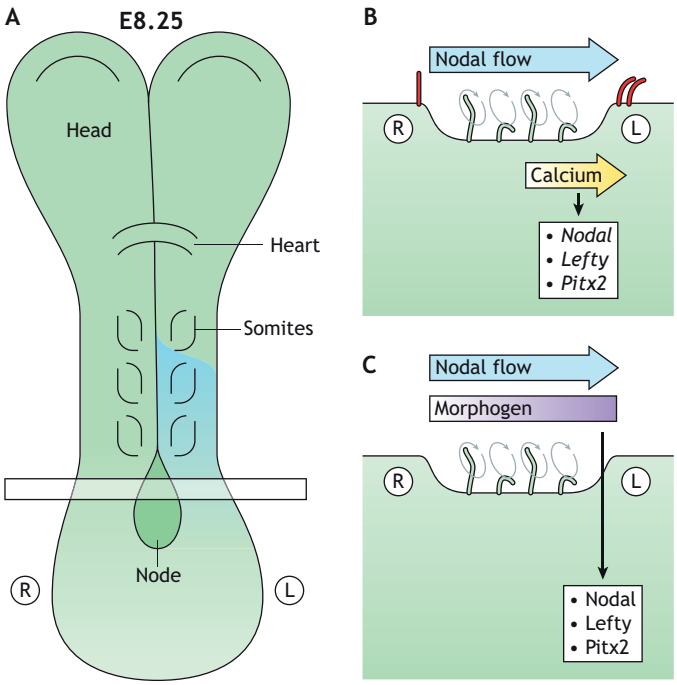

Fig. 2. Mechanosensation versus chemosensation theories of nodal flow. (A) Schematic overview of E8.25 mouse embryo; Nodal (blue) is expressed on the left side. Horizontal box indicates the plane of the cross-section through the node displayed in B and C. (B) In the mechanosensation model, cilia-driven Nodal flow is sensed by immotile mechanosensitive cilia (red), which induces an intracellular Ca^{2+} increase and stimulates Nodal, Lefty and Pitx2 expression. (C) In the chemosensation model, cilia-driven Nodal flow creates a morphogen gradient towards the left side of the node, where receptor-based signalling induces *Nodal*, *Lefty* and *Pitx2* expression. L, left; R, right. Based on data from Tabin and Vogan (2003).

Development (2020) 147, dev185579. doi:10.1242/dev.185579

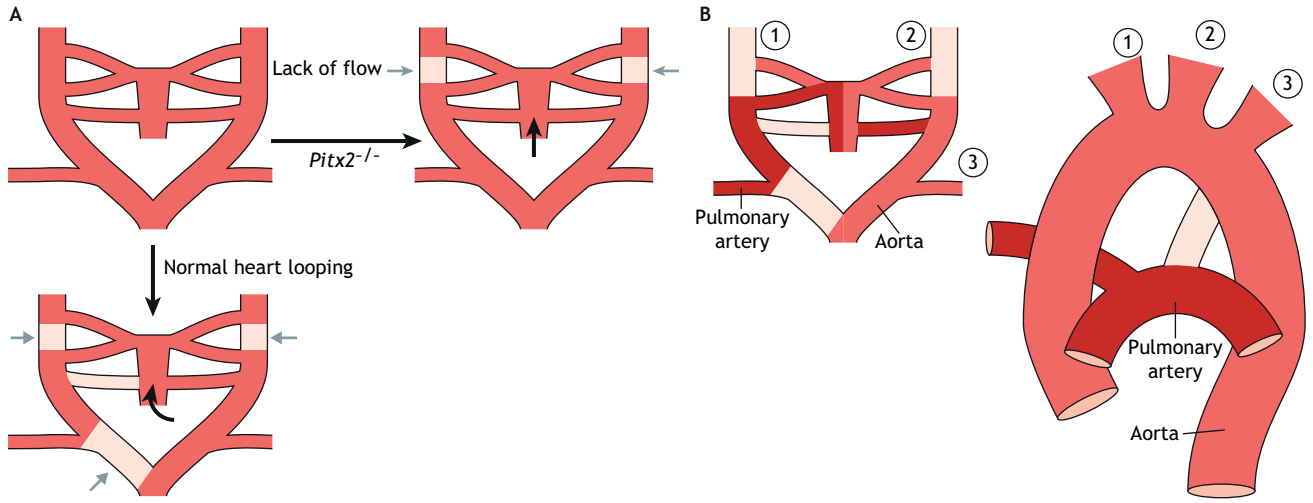

Fig. 3. Flow-dependent cardiac looping and aortic arch selection. (A) Schematic overview of the effects of cardiac looping on aortic arch selection. When heart looping occurs normally (left), blood (red) flows into the pharyngeal arches in a twisting motion, as indicated by the black arrow, and the pharyngeal arch that experiences the lowest flow regresses, as indicated by the grey arrows. In *Pitx2*$^{-/-}$ mutants (right), the heart fails to initiate looping and blood flow enters the pharyngeal arches straight, as indicated by the black arrow. As a result, blood flow remains constant in all arches. (B) Schematic overview demonstrating how the pharyngeal arches remodel into the aorta and pulmonary artery. 1, brachiocephalic artery; 2, left common carotid artery; 3, left subclavian artery.

each other in low shear stress regions (Djonov et al., 2002; Karthik et al., 2018) (Fig. 5B).

The developing vasculature produces an excess of vessels that are then pruned by selective regression. Vessels experiencing sufficiently high shear stresses are maintained, whereas those unable to meet this threshold regress (Chen et al., 2012; de Jong et al., 2012; Kochhan et al., 2013; Korn and Augustin, 2015). In well-perfused vessels, endothelial cells elongate and align with flow; their Golgi apparatus is located upstream of the nucleus, polarising the cell against the flow (Franco et al., 2015). During vessel regression in low flow vessels, axial polarity is misaligned, after which these endothelial cells actively migrate out of the regressing vessel segment to contribute to higher flow segments (Chen et al., 2012; Franco et al., 2015; Udan et al., 2013) (Fig. 5C).

Vascular fusion, or reverse-intussusception, is a major method of vessel enlargement during development (Chouinard-Pelletier et al., 2013; Udan et al., 2013). During fusion, smaller vessels merge to share one lumen, thereby increasing the diameter of a vessel rapidly. Vascular fusion occurs in regions of high flow but is driven by low shear stress levels (Chouinard-Pelletier et al., 2013). Avascular pillars that disturb the flow stream create a low shear stress downstream of the avascular region. VE-Cadherin phosphorylation

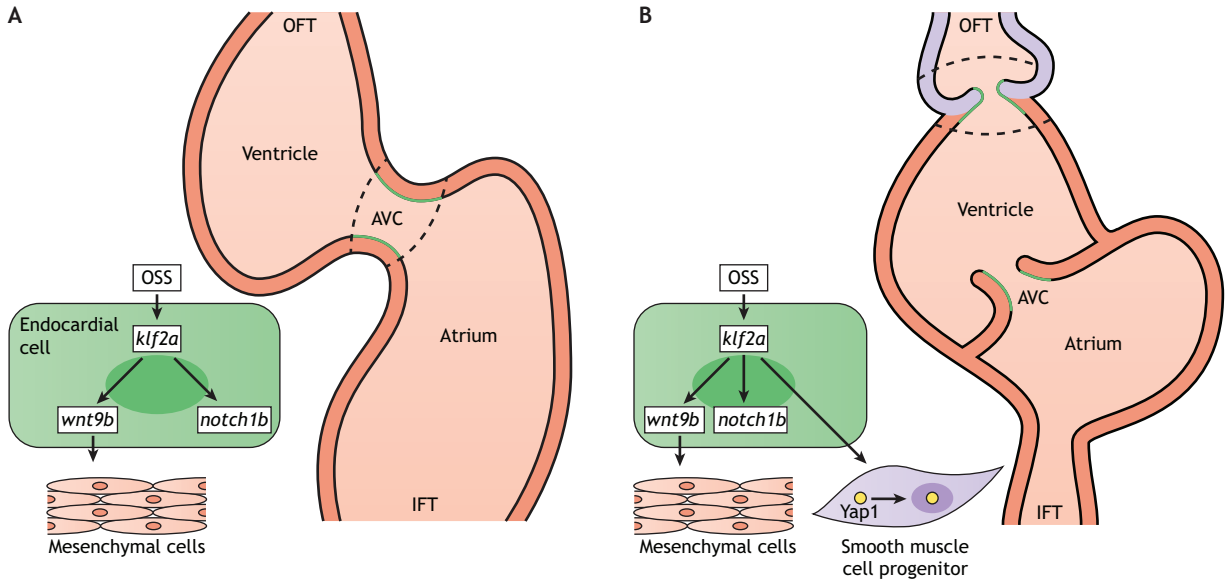

Fig. 4. Cardiac valve development is dependent on oscillatory flow in zebrafish embryos. (A) At 48 hpf, the zebrafish heart consists of one atrium and one ventricle, with the atrioventricular canal (AVC) channel in between and blood flows from the inflow tract (IFT) to the outflow tract (OFT). At the AVC channel, oscillatory shear stress (OSS) induces *klf2a* expression in the lining endocardial cells (green). OSS-induced *klf2a* stimulates endocardial *notch1b* expression, which is necessary for rearrangement of cardiac valve leaflet cells, and *wnt9b* expression, which stimulates cardiac cushion remodelling in the underlying mesenchymal cells. (B) At 96 hpf, the AVC valve is established and the OFT valve starts to form. OSS-induced *klf2a* expression in endocardial cells also induces *notch1b* and *wnt9b* expression. Moreover, endocardial *klf2a* expression stimulates Yap1 nuclearisation in the surrounding smooth muscle cell progenitors.

Development (2020) 147, dev185579. doi:10.1242/dev.185579

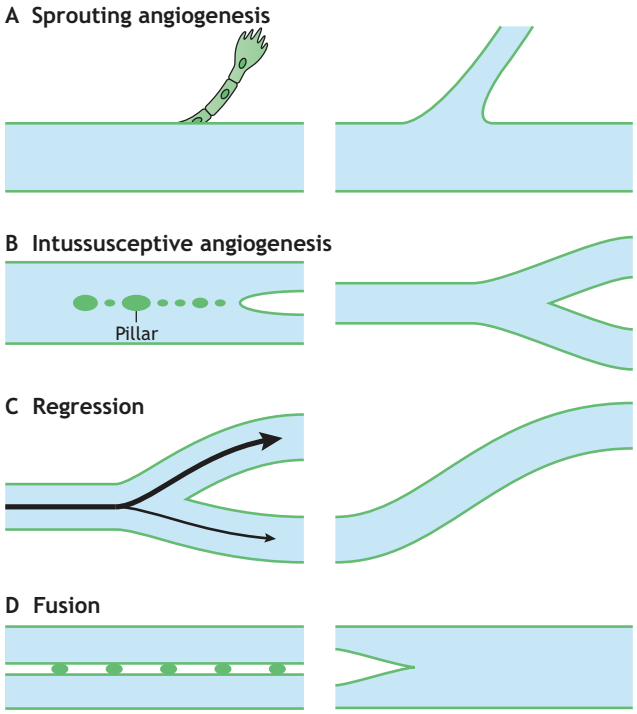

Fig. 5. Vascular remodelling is dependent on shear stress in mammals. (A) Sprouting angiogenesis occurs at a shear stress minimum. (B) In intussusceptive angiogenesis pillars form in areas of high flow but fuse at the lowest shear stress. (C) Regression occurs in vessels with low flow. (D) Fusion of vessels occurs in regions of low shear stress and contributes to formation of the major vessels. Endothelial cells are in green; vessel lumen is in blue.

occurs in these low shear stress regions and rearranges the junctional complexes of endothelial cells, allowing two nearby vessels to fuse (Caolo et al., 2018) (Fig. 5D).

In the final phase of vascular remodelling, smooth muscle cells and pericytes are recruited to stabilise the vasculature, a process facilitated by a number of mechanosensitive pathways. The G protein-coupled S1P receptor 1 (S1PR1) governs pericyte and smooth muscle cell recruitment during embryonic development and is activated by laminar shear stress (LSS) (Gaengel et al., 2009; Jung et al., 2012). In the absence of S1P1, flow-mediated signalling is reduced in endothelial cells *in vitro*, and *S1p1*$^{-/-}$ embryos present with vascular leakage and dysregulated blood flow (Jung et al., 2012). Furthermore, in zebrafish embryos, shear stress sensed through primary cilia activates the Notch signalling pathway in arterial endothelial cells and promotes *Foxc1b* expression (Chen et al., 2017). *Foxc1b* drives vascular smooth muscle cell recruitment by activating mesodermal cells present in close proximity to arterial-fated vessels (Chen et al., 2017). After recruitment of pericytes, interaction between endothelial cells and pericytes is stimulated by flow-mediated miR-27b, which inhibits semaphorin expression and accompanied repulsive signals (Demolli et al., 2017).

Besides shear stress, blood flow also creates a circumferential stretch, induced by the beating heart. Stretch requires a vessel to be elastic. Hydrostatic pressure, the absolute level of pressure, is not extremely biologically active. Rather, the biologically stronger signal is the expansion and contraction that occurs as elastic vessels are exposed to pulse pressure. Much less is known about the role of stretch compared with shear stress, and *in vivo*, it is extremely difficult to separate the two. Several mechanosensitive Ca^{2+} channels, including Piezo1 and Trpp2, are stretch-activated channels. However, shear stress also creates tension on endothelial cell membranes, similar to the effects of stretch. This makes it difficult to assess whether the major role of these channels *in vivo* relates to sensing shear stress or stretch (Melchior and Frangos, 2010; Yamamoto and Ando, 2013).

Haematopoiesis

Between E6.5 and E9.0 of mouse development, the first blood cells (both erythroid and myeloid cells) form in the extra-embryonic yolk sac (Kasaai et al., 2017; Samokhvalov et al., 2007; Tanaka et al., 2012; Yoder et al., 1997). Later, HSCs emerge from the aorta-gonad-mesonephros (AGM) region, before colonising liver and finally bone marrow (Medvinsky and Dzierzak, 1996; Müller et al., 1994; Yokomizo and Dzierzak, 2010). Time-lapse imaging has demonstrated that HSCs can derive directly from specialised aortic endothelium called the ‘haemogenic endothelium’ (Lam et al., 2010; reviewed by Adamo and García-Cardeña, 2012). Given their vascular localisation, haemogenic endothelium and differentiating and emerging HSCs are exposed to the same forces of flow as vascular endothelial cells.

Shear stress-driven nitric oxide (NO) production is crucial for the formation and release of HSCs into the circulation of the embryo. In the absence of blood flow, there is a severe reduction of circulating HSCs in the zebrafish embryo (North et al., 2009). Shear stress activates *klf2a* expression in haemogenic endothelium, where it promotes the expression of *nos1/2b*, thus increasing NO production (Adamo et al., 2009; Wang et al., 2011b). If NO production is blocked, fewer haemogenic cells are present in the AGM region at E10.5, even if blood flow remains (Adamo et al., 2009). Similarly, in the zebrafish embryo, either the loss of *klf2a* expression or loss of heartbeat results in reduced expression of *Runx1*, an important regulator of haematopoiesis, a phenotype rescued by external NO delivery (North et al., 2009; Wang et al., 2011b). Shear stress also induces the expression of *RUNX1* and Yap1 nuclearisation in induced pluripotent stem cell-derived haemogenic endothelial cells *in vitro* (Lundin et al., 2020). Moreover, in zebrafish embryos, haemodynamic-driven Yap1 nuclearisation supports HSC specification and maturation, independent of the usual hippo signalling activation (Lundin et al., 2020; Nakajima et al., 2017).

Lymph flow

Lymphatic endothelial cells (LECs) that line lymphatic vessels are highly sensitive to the low levels of shear stress created by lymph flow (Baeyens et al., 2015). VEGFR3, a component of the junctional mechanosensory complex is abundantly expressed on LECs and specifically tunes the high sensitivity of LECs to the low shear stresses of lymph flow (Baeyens et al., 2015). The mechanosensitive protein FOXC2 and its upstream regulators β-catenin and GATA2 are necessary for the stabilisation of the developing lymphatic vasculature (Cha and Srinivasan, 2016; Sabine et al., 2015; Sweet et al., 2015). Furthermore, increased LSS induces sprouting in LECs, likely reflecting the need for increased draining in high lymph flow regions (Choi et al., 2017).

Lymphatic valve formation

Lymph flow also drives lymphatic valve formation as lymphatic valves are absent in mouse embryos that lack lymph flow due to loss of C-type lectin-like receptor 2 (Clec2), where lymph flow is opposed by the backflow of blood (Sweet et al., 2015). Lymphatic valves form in areas of maximal OSS, where Prox1 and subsequently Foxc2 expression are highest. Here, OSS induces Wnt/β-catenin signalling, which in turn controls Foxc2 expression (Sabine et al., 2012). As Foxc2 has a slightly different expression

pattern than Prox1, the up- and downstream valve leaflet surfaces become distinct (Cha et al., 2016; Sabine et al., 2012) (Fig. 6B). Moreover, Prox1 and Foxc2 together modulate Cx37 expression, which in turn regulates Nfatc1 signalling, a crucial pathway for the maturation and stabilisation of lymphatic valves (Sabine et al., 2012) (Fig. 6C). As the valves mature, Cx37 expression is driven particularly by the recirculating flow downstream of elongating leaflets of the lymphatic valves (Sabine et al., 2012), which further stimulates the differentiation of lymphatic valves. Endothelial-specific deletion of *Piezo1* impairs lymphatic valve protrusion (Nonomura et al., 2018). However, loss of *Piezo1* does not disrupt expression of Prox1, Foxc2 or Nfatc1 at valve forming regions, suggesting that Piezo1 functions in a separate molecular pathway, likely related to cytoskeletal re-organisation (Nonomura et al., 2018).

Lymph node development

Lymph flow is necessary for the expansion and maturation of the lymph node. Primordial lymph nodes form by E16.5 (Blum and Pabst, 2006; van de Pavert and Mebius, 2010). Interstitial lymph flows through the developing lymph node and amplifies Cxcl13 expression, promotes the retention of inducer cells and is necessary for the formation of the subcapsular sinus, as well as for recruitment of macrophages to the sinus (Bovay et al., 2018). In the absence of FOXC2, lymphatic valves fail to form, so that unidirectional lymphatic flow does not occur (Petrova et al., 2004). Instead, lymphatic flow remains bidirectional, preventing lymph node maturation as inducer cells are not retained within the forming lymph node (Bovay et al., 2018).

Cerebrospinal fluid flow

During early development, the neural tube closes and bends to form three fluid-filled cavities: the X, Y and telencephalic ventricles (Lowery and Sive, 2009). In amphibians and mammals, the telencephalic ventricle further matures into two lateral ventricles to form four ventricles in the adult brain (Lowery and Sive, 2009). During early embryonic development, these cavities are already filled with cerebrospinal fluid (CSF), secreted by the choroid plexuses, after which it enters the spinal cord. Here, we present the key concepts in CSF flow, focussing on development (extensively reviewed by Fame and Lehtinen, 2020; Ringers et al., 2020).

Brain ventricular system

CSF flow in the brain ventricles consists of a macrofluidic component, which makes up the bulk of flow in the middle of the ventricles, and a microfluidic component close to the ventricle wall (Ringers et al., 2020; Siyahhan et al., 2014). The major bulk of flow is driven by a number of cues, such as the pressure gradient created by CSF secretion, exchange of CSF with interstitial fluid, cardiac and respiratory cycles, and even body movements, which therefore make CSF flow difficult to study (Dreha-Kulaczewski et al., 2015; Feinberg and Mark, 1987; Olstad et al., 2019; Ringers et al., 2020; Spassky et al., 2005; Xu et al., 2016). The bulk CSF flow is primarily thought to nourish the brain and maintain brain homeostasis (Ringers et al., 2020).

Microfluidic flow close to the ventricle wall has been studied more extensively during development and is at least partly supported by motile cilia present on ependymal cells lining the ventricle, as demonstrated in zebrafish (Grimes et al., 2016; Olstad et al., 2019), mice (Abdelhamed et al., 2018; Banizs et al., 2005; Ibañez-Tallon et al., 2004), pigs (Faubel et al., 2016) and humans (Worthington and Cathcart, 1966). In both zebrafish and mouse, insufficient CSF flow due to impaired ciliary motility, as well as deficient mechanosensation, induces ventricular defects and eventually hydrocephalus: an enlargement of the brain ventricles (Banizs et al., 2005; Grimes et al., 2016; Ibañez-Tallon et al., 2004; Kramer-Zucker et al., 2005). For example, the dynein-complex driving cilia motion contains Dnah5; *Dnah5*$^{-/-}$ mice lack CSF flow and develop hydrocephalus during early postnatal development (Ibañez-Tallon, 2002; Ibañez-Tallon et al., 2004). Similarly, mutations disrupting intraflagellar transport, such as *Ift88*$^{-/-}$ and *Ift57*$^{-/-}$ in mouse embryos, affect proper formation of both motile and mechanosensory cilia, causing hydrocephalus (Banizs et al., 2005; Kramer-Zucker et al., 2005). However, individuals with primary ciliary dyskinesia barely present with hydrocephalus (Lee, 2013), which suggests apparent differences between species. These differences could possibly be explained by the difference in ventricular size, which could change the contribution of bulk CSF flow compared with near-wall CSF flow (Ringers et al., 2020).

Radial glia cells are neuronal stem cells in the subventricular zone, which is located beneath the ependyma of the lateral ventricle, that give rise to neurons, glia cells and ependymal cells. Ependymal cells arise from radial glia (Spassky et al., 2005). Ependymal cells are multi-ciliated cells that drive CSF flow and, as with the LRO, the polarisation of these cells is important for their function. Translational polarity is defined by the position of the basal bodies on the apical surface of the cell, while rotational polarity is defined by the angle of individual basal bodies (Mirzadeh et al., 2010). Before ependymal cells arise, radial glia cells have already initiated the well-defined ependymal PCP in mice through mechanosensation (Mirzadeh et al., 2010; Ohata et al., 2016) (Fig. 7). The mechanosensors Trpp1 and Trpp2 on the primary cilia sense CSF flow in the embryonic ventricles, driving translational polarity in mice (Guirao et al., 2010; Mirzadeh et al., 2010; Ohata

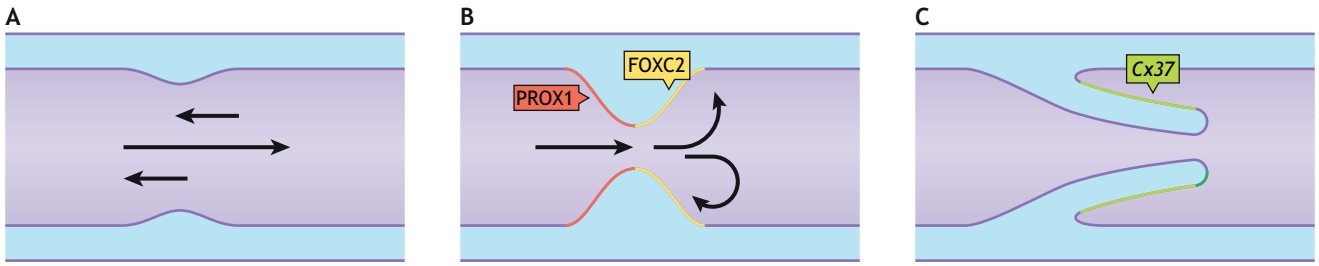

Fig. 6. The formation of lymphatic valves is dependent on oscillatory flow. (A) Lymph (lilac) flows bidirectionally in the absence of valves. (B) Valve territory is established where oscillatory shear stress (OSS) peaks. OSS induces PROX1 and FOXC2 expression. Small differences in expression patterns mark the different valve leaflets. (C) PROX1 and FOXC2 induce *Cx37* expression in the established valve, which is required for leaflet formation and stabilisation. Endothelial cells are in dark purple; lymphatic lumen is in light purple; mesenchymal cells are in blue.

Development (2020) 147, dev185579. doi:10.1242/dev.185579

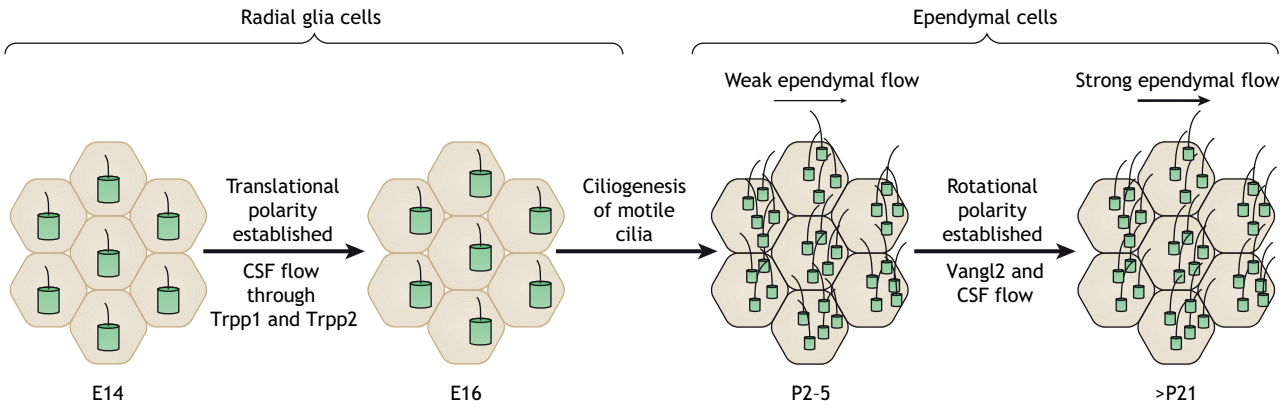

Fig. 7. The correct alignment of ependymal cells in the brain ventricles is dependent on CSF flow in mouse embryos. During late embryonic development, radial glia cells equipped with a primary cilium (green) are randomly dispersed. Mechanosensors Trpp1 and Trpp2 sense CSF flow and initiate a translational polarity, which is established around E16.0 and is conserved through differentiation into ependymal cells. Shortly after birth, ependymal cells undergo extensive ciliogenesis, resulting in a number of motile cilia (green). A weak ependymal flow is initiated by these motile cilia, which grows into a strong and unidirectional flow once rotational polarity is established through Vangl2 and a positive-feedback loop of CSF flow. Based on data from Ohata et al. (2016).

et al., 2015). This translational polarity is preserved when they undergo differentiation into ependymal cells postnatally, which is accompanied by extensive ciliogenesis. Ependymal cells have multiple motile cilia, which gradually align with CSF flow (Guirao et al., 2010). This rotational polarity is regulated through Vangl2 and a positive-feedback loop of CSF flow, as evidenced from cultured ependymal cells, although it remains unclear how these motile cilia sense CSF flow (Guirao et al., 2010; Mitchell et al., 2007; Ohata et al., 2016). Furthermore, Trpp1 and Trpp2 govern a balance between proliferation and differentiation of radial glia cells in mice (Winokurow and Schumacher, 2019). Loss of *Trpp1* or *Trpp2* stimulates increased proliferation of radial glia cells through Notch signalling and Stat3, while impairing their differentiation to neurons (Winokurow and Schumacher, 2019).

Besides direct mechanosensory effects, CSF flow has long been thought to transport molecules and fine-tune the distribution of molecules in the lateral ventricles and the spinal cord. For example, bulk CSF flow guides the migration of newly formed neuroblasts in the adult mouse brain by creating a gradient of chemo-repulsive molecules, such as Slit proteins (Sawamoto et al., 2006). Similarly, Wnt5a is secreted by the choroid plexuses and is guided by CSF flow towards neural progenitors, supporting cerebellar development (Kaiser et al., 2019). Moreover, when ciliary motility is impaired either in brain or spinal cord, none of the beads injected in the ventricles is transported into the central canal of the spinal cord, suggesting that ciliary motility controls long-range CSF transport (Thouvenin et al., 2020).

Spinal cord

In the spinal cord, motile cilia are present on floor plate cells, ependymal cells that line the central canal, and CSF-contacting neurons. Motile cilia in the spinal cord have been discovered in a number of species, including zebrafish, chick, mice, rats and humans, but have been most extensively studied in zebrafish.

In 24-30 h post fertilisation (hpf) zebrafish embryos, CSF flows bidirectionally through the spinal cord (Cantaut-Belarif et al., 2018; Sternberg et al., 2018; Thouvenin et al., 2020). Motile cilia primarily line the ventral wall of the central canal of zebrafish embryos, allowing for an asymmetric distribution and, consequently, a bidirectional CSF flow (Thouvenin et al., 2020). This bidirectional CSF flow is enhanced by contractions of the body wall muscles (Olstad et al., 2019; Thouvenin et al., 2020). Additionally, proper ciliary movement drives the formation of the lumen of the central canal, as zebrafish mutants with impaired ciliary motility present with a reduced diameter of the central canal (Thouvenin et al., 2020).

In zebrafish, impaired ciliary motility is often accompanied by improper straightening of the spine (Grimes et al., 2016; Sternberg et al., 2018; Zhang et al., 2018). Straightening of the spine is dependent on the formation of Reissner's fibre, a thread composed of subcommissural organ (SCO)-spondin proteins that are secreted into the central canal of the spinal cord by the SCO (Cantaut-Belarif et al., 2018). Both CSF flow and ciliary motility are necessary for the formation and secretion of Reissner's fibre (Cantaut-Belarif et al., 2018). CSF flow also transports adrenaline from the brain towards the spinal cord of zebrafish embryos, where it stimulates the release of urotensin neuropeptides Urp1 and Urp2 from CSF-contacting neurons (Zhang et al., 2018). The secreted neuropeptides activate slow-twitch muscle fibres and the subsequent contractions are hypothesised to straighten the spinal cord in zebrafish embryos (Sternberg et al., 2018; Zhang et al., 2018). Last, CSF-contacting neurons are equipped with the mechanosensory Trpp2l1 Ca^{2+} channel, which enables them to react directly to CSF flow (Sternberg et al., 2018). Either loss of *Trpp2l1*, impaired ciliary motility or obstructed urotensin neuropeptide secretion results in severe scoliosis of the zebrafish adult (Sternberg et al., 2018; Zhang et al., 2018). CSF flow and ciliary motility remain important during adulthood to ensure spine straightening, as scoliosis is observed even when motile cilia function is impaired at post-embryonic stages (Buchan et al., 2014; Grimes et al., 2016; Konjikusic et al., 2018). In humans, CSF flow is impaired in individuals with Chiari malformations that suffer from scoliosis and individuals with primary ciliary dyskinesia, who also present with scoliosis (Engesaeth et al., 1993; McGirt et al., 2008; Panigrahi et al., 2004).

Conclusions

Mechanosensitive signalling in response to flow elicits important structural adaptations in the developing embryo. However, mechanosensing is not limited to fluid flow exerted directly onto luminal cells. Other physical forces modulate early embryonic shape changes, later tissue folding events and even musculoskeletal development (Anlaş and Nelson, 2018; Arvind and Huang, 2017; Heer and Martin, 2017). Moreover, the importance of fluid flow is

not limited to embryonic development, and is crucial to the progression of many diseases such as atherosclerosis (Souilhol et al., 2019). There is much to learn both from the similarities and the differences between organ systems and developmental stages regarding the role of flow in morphogenesis.

Competing interests
The authors declare no competing or financial interests.

Funding
H.M.P. was supported by a fellowship from the Fonds Wetenschappelijk Onderzoek (11ZD516N). E.A.V.J. and M.D. were supported by C1 internal KU Leuven funding (C14/19/095). E.A.V.J. was supported by a research grant from the Fonds Wetenschappelijk Onderzoek (G091018N and G0B5920N) and a research grant from Horizon 2020 (848109).

References

Abdelhamed, Z., Vuong, S. M., Hill, L., Shula, C., Timms, A., Beier, D., Campbell, K., Mangano, F. T., Stottmann, R. W. and Goto, J. (2018). A mutation in Ccdc39 causes neonatal hydrocephalus with abnormal motile cilia development in mice. *Development (Camb.)* **145**, dev154500. doi:10.1242/dev.154500

Aboualaiwi, W. A., Takahashi, M., Mell, B. R., Jones, T. J., Ratnam, S., Kolb, R. J. and Nauli, S. M. (2009). Ciliary polycystin-2 is a mechanosensitive calcium channel involved in nitric oxide signaling cascades. *Circ. Res.* **104**, 860-869. doi:10.1161/CIRCRESAHA.108.192765

Adamo, L. and García-Cardeña, G. (2012). The vascular origin of hematopoietic cells. *Dev. Biol.* **362**, 1-10. doi:10.1016/j.ydbio.2011.09.008

Adamo, L., Naveiras, O., Wenzel, P. L., McKinney-Freeman, S., Mack, P. J., Gracia-Sancho, J., Suchy-Dicey, A., Yoshimoto, M., Lensch, M. W., Yoder, M. C. et al. (2009). Biomechanical forces promote embryonic haematopoiesis. *Nature* **459**, 1131-1135. doi:10.1038/nature08073

Akbari, E., Spychalski, G. B., Rangharajan, K. K., Prakash, S. and Song, J. W. (2019). Competing fluid forces control endothelial sprouting in a 3-D microfluidic vessel bifurcation model. *Micromachines* **10**, 451. doi:10.3390/mi10070451

Al-Roubaie, S., Jahnsen, E. D., Mohammed, M., Henderson-Toth, C. and Jones, E. A. V. (2011). Rheology of embryonic avian blood. *Am. J. Physiol. Heart Circ. Physiol.* **301**, H2473-H2481. doi:10.1152/ajpheart.00475.2011

Anlaş, A. A. and Nelson, C. M. (2018). Tissue mechanics regulates form, function, and dysfunction. *Curr. Opin. Cell Biol.* **54**, 98-105. doi:10.1016/j.ceb.2018.05.012

Arvind, V. and Huang, A. H. (2017). Mechanobiology of limb musculoskeletal development. *Ann. N. Y. Acad. Sci.* **1409**, 18-32. doi:10.1111/nyas.13427

Auman, H. J., Coleman, H., Riley, H. E., Olale, F., Tsai, H. J. and Yelon, D. (2007). Functional modulation of cardiac form through regionally confined cell shape changes. *PLoS Biol.* **5**, e53. doi:10.1371/journal.pbio.0050053

Baeyens, N., Nicoli, S., Coon, B. G., Ross, T. D., Van Den Dries, K., Han, J., Lauridsen, H. M., Mejean, C. O., Eichmann, A., Thomas, J. L. et al. (2015). Vascular remodeling is governed by a vegfr3-dependent fluid shear stress set point. *eLife* **4**, 1-35. doi:10.7554/eLife.04645

Baeyens, N., Larrivée, B., Ola, R., Hayward-Piatkowskyi, B., Dubrac, A., Huang, B., Ross, T. D., Coon, B. G., Min, E., Tsarfati, M. et al. (2016). Defective fluid shear stress mechanotransduction mediates hereditary hemorrhagic telangiectasia. *J. Cell Biol.* **214**, 807-816. doi:10.1083/jcb.201603106

Banizs, B., Pike, M. M., Millican, C. L., Ferguson, W. B., Komlosi, P., Sheetz, J., Bell, P. D., Schwiebert, E. M. and Yoder, B. K. (2005). Dysfunctional cilia lead to altered ependyma and choroid plexus function, and result in the formation of hydrocephalus. *Development* **132**, 5329-5339. doi:10.1242/dev.02153

Banjo, T., Grajcarek, J., Yoshino, D., Osada, H., Miyasaka, K. Y., Kida, Y. S., Ueki, Y., Nagayama, K., Kawakami, K., Matsumoto, T. et al. (2013). Haemodynamically dependent valvulogenesis of zebrafish heart is mediated by flow-dependent expression of miR-21. *Nat. Commun.* **4**, 1-11. doi:10.1038/ncomms2978

Bazigou, E., Xie, S., Chen, C., Weston, A., Miura, N., Sorokin, L., Adams, R., Muro, A. F., Sheppard, D. and Makinen, T. (2009). Integrin-α9 is required for fibronectin matrix assembly during lymphatic valve morphogenesis. *Dev. Cell* **17**, 175-186. doi:10.1016/j.devcel.2009.06.017

Bernabeu, M. O., Jones, M. L., Nielsen, J. H., Krüger, T., Nash, R. W., Groen, D., Schmieschek, S., Hetherington, J., Gerhardt, H., Franco, C. A. et al. (2014). Computer simulations reveal complex distribution of haemodynamic forces in a mouse retina model of angiogenesis. *J. R. Soc. Interface* **11**, 20140543. doi:10.1098/rsif.2014.0543

Blum, M. and Ott, T. (2018). Animal left–right asymmetry. *Curr. Biol.* **28**, R301-R304. doi:10.1016/j.cub.2018.02.073

Blum, K. S. and Pabst, R. (2006). Keystones in lymph node development. *J. Anat.* **209**, 585-595. doi:10.1111/j.1469-7580.2006.00650.x

Borovina, A., Superina, S., Voskas, D. and Ciruna, B. (2010). Vangl2 directs the posterior tilting and asymmetric localization of motile primary cilia. *Nat. Cell Biol.* **12**, 407-412. doi:10.1038/ncb2042

Boselli, F., Steed, E., Freund, J. B. and Vermot, J. (2017). Anisotropic shear stress patterns predict the orientation of convergent tissue movements in the embryonic heart. *Development* **144**, 4322-4327. doi:10.1242/dev.152124

Bovay, E., Sabine, A., Prat-Luri, B., Kim, S., Son, K., Willrodt, A.-H., Olsson, C., Halin, C., Kiefer, F., Betsholtz, C. et al. (2018). Multiple roles of lymphatic vessels in peripheral lymph node development. *J. Exp. Med.* **215**, 2760-2777. doi:10.1084/jem.20180217

Buchan, J. G., Gray, R. S., Gansner, J. M., Alvarado, D. M., Burgert, L., Gitlin, J. D., Gurnett, C. A. and Goldsmith, M. I. (2014). Kinesin family member 6 (kif6) is necessary for spine development in zebrafish: KIF6 in Zebrafish Spine Development. *Dev. Dyn.* **243**, 1646-1657. doi:10.1002/dvdy.24208

Burri, P. H. and Djonov, V. (2002). Intussusceptive angiogenesis—the alternative to capillary sprouting. *Mol. Asp. Med.* **23**, 1-27. doi:10.1016/S0098-2997(02)00096-1

Cantaut-Belarif, Y., Sternberg, J. R., Thouvenin, O., Wyart, C. and Bardet, P. L. (2018). The reissner fiber in the cerebrospinal fluid controls morphogenesis of the body axis. *Curr. Biol.* **28**, 2479-2486.e4. doi:10.1016/j.cub.2018.05.079

Caolo, V., Peacock, H. M., Kasaai, B., Swennen, G., Gordon, E., Claesson-Welsh, L., Post, M. J., Verhamme, P. and Jones, E. A. V. (2018). Shear stress and VE-cadherin: the molecular mechanism of vascular fusion. *Arterioscler. Thromb. Vasc. Biol.* **38**, 2174-2183. doi:10.1161/ATVBAHA.118.310823

Cartwright, J. H. E., Piro, O. and Tuval, I. (2004). Fluid-dynamical basis of the embryonic development of left-right asymmetry in vertebrates. *Proc. Natl. Acad. Sci. USA* **101**, 7234-7239. doi:10.1073/pnas.0402001101

Cartwright, J. H. E., Piro, O. and Tuval, I. (2020). Chemosensing versus mechanosensing in nodal and Kupffer's vesicle cilia and in other left–right organizer organs. *Philos. Trans. R. Soc. B Biol. Sci.* **375**, 20190566. doi:10.1098/rstb.2019.0566

Cha, B. and Srinivasan, R. S. (2016). Mechanosensitive β-catenin signaling regulates lymphatic vascular development. *BMB Rep.* **49**, 403-404. doi:10.5483/BMBRep.2016.49.8.112

Cha, B., Geng, X., Mahamud, M. R., Fu, J., Mukherjee, A., Kim, Y., Jho, E.-H. H., Kim, T. H., Kahn, M. L., Xia, L. et al. (2016). Mechanotransduction activates canonical Wnt/β-catenin signaling to promote lymphatic vascular patterning and the development of lymphatic and lymphovenous valves. *Genes Dev.* **30**, 1454-1469. doi:10.1101/gad.282400.116

Cha, B., Geng, X., Mahamud, M. R., Zhang, J. Y., Chen, L., Kim, W., Jho, E. H., Kim, Y., Choi, D., Dixon, J. B. et al. (2018). Complementary Wnt sources regulate lymphatic vascular development via PROX1-dependent Wnt/β-catenin signaling. *Cell Rep.* **25**, 571-584.e5. doi:10.1016/j.celrep.2018.09.049

Chapman, W. B. (1918). The effect of the heart-beat upon the development of the vascular system in the chick. *Am. J. Anat.* **23**, 175-203. doi:10.1002/aja.1000230107

Chen, Q., Jiang, L., Li, C., Hu, D., Bu, J. W., Cai, D. and Du, J. L. (2012). Haemodynamics-driven developmental pruning of brain vasculature in zebrafish. *PLoS Biol.* **10**, e1001374. doi:10.1371/journal.pbio.1001374

Chen, X., Gays, D., Milia, C. and Santoro, M. M. (2017). Cilia control vascular mural cell recruitment in vertebrates. *Cell Rep.* **18**, 1033-1047. doi:10.1016/j.celrep.2016.12.044

Chiang, I. K.-N., Fritzsche, M., Pichol-thievend, C., Neal, A., Holmes, K., Lagendijk, A., Overman, J., D'Angelo, D., Omini, A., Hermkens, D. et al. (2017). SoxF factors induce Notch1 expression via direct transcriptional regulation during early arterial development(Development, (2017), 144, (2629-2639), 10.1242/dev.146241). *Development* **144**, 3847-3848. doi:10.1242/dev.159715

Choi, D., Park, E., Jung, E., Seong, Y. J., Yoo, J., Lee, E., Hong, M., Lee, S., Ishida, H., Burford, J. et al. (2017). Laminar flow downregulates Notch activity to promote lymphatic sprouting. *J. Clin. Investig.* **127**, 1225-1240. doi:10.1172/JCI87442

Chong, D. C., Koo, Y., Xu, K., Fu, S. and Cleaver, O. (2011). Stepwise arteriovenous fate acquisition during mammalian vasculogenesis. *Dev. Dyn.* **240**, 2153-2165. doi:10.1002/dvdy.22706

Chouinard-Pelletier, G., Jahnsen, E. D. and Jones, E. A. V. (2013). Increased shear stress inhibits angiogenesis in veins and not arteries during vascular development. *Angiogenesis* **16**, 71-83. doi:10.1007/s10456-012-9300-2

Corrigan, M. A., Johnson, G. P., Stavenschi, E., Riffault, M., Labour, M.-N. and Hoey, D. A. (2018). TRPV4-mediates oscillatory fluid shear mechanotransduction in mesenchymal stem cells in part via the primary cilium. *Sci. Rep.* **8**, 1-13. doi:10.1038/s41598-018-22174-3

Corti, P., Young, S., Chen, C.-Y., Patrick, M. J., Rochon, E. R., Pekkan, K. and Roman, B. L. (2011). Interaction between alk1 and blood flow in the development of arteriovenous malformations. *Development* **138**, 1573-1582. doi:10.1242/dev.060467

de Jong, O. G., Verhaar, M. C., Chen, Y., Vader, P., Gremmels, H., Posthuma, G., Schiffelers, R. M., Gucek, M. and van Balkom, B. W. M. (2012). Cellular stress conditions are reflected in the protein and RNA content of endothelial cell-derived exosomes. *J. Extracellular Vesicles* **1**, 18396. doi:10.3402/jev.v1i0.18396

Dekker, R. J., Van Soest, S., Fontijn, R. D., Salamanca, S., De Groot, P. G., Vanbavel, E., Pannekoek, H., Horrevoets, A. J. G. G., Soest, S. Van et al. (2002). Prolonged fluid shear stress induces a distinct set of endothelial cell

genes, most specifically lung Kruppel-like factor (KLF2). *Blood* **100**, 1689-1698. doi:10.1182/blood-2002-01-0046

Dellinger, M., Hunter, R., Bernas, M., Gale, N., Yoncopoulos, G., Erickson, R. and Witte, M. (2008). Defective remodeling and maturation of the lymphatic vasculature in Angiopoietin-2 deficient mice. *Dev. Biol.* **319**, 309-320. doi:10.1016/j.ydbio.2008.04.024

Demolli, S., Doddaballapur, A., Devraj, K., Stark, K., Manavski, Y., Eckart, A., Zehendner, C. M., Lucas, T., Korff, T., Hecker, M. et al. (2017). Shear stress-regulated miR-27b controls pericyte recruitment by repressing SEMA6A and SEMA6D. *Cardiovasc. Res.* **113**, 681-691. doi:10.1093/cvr/cvx032

Dietrich, A.-C. C., Lombardo, V. A., Veerkamp, J., Priller, F. and Abdelilah-Seyfried, S. (2014). Blood flow and Bmp signaling control endocardial chamber morphogenesis. *Dev. Cell* **30**, 367-377. doi:10.1016/j.devcel.2014.06.020

Dinsmore, C. and Reiter, J. F. (2016). Endothelial primary cilia inhibit atherosclerosis. *EMBO Rep.* **17**, 156-166. doi:10.15252/embr.201541019

Djonov, V. G., Kurz, H. and Burri, P. H. (2002). Optimality in the developing vascular system: Branching remodeling by means of intussusception as an efficient adaptation mechanism. *Dev. Dyn.* **224**, 391-402. doi:10.1002/dvdy.10119

Dreha-Kulaczewski, S., Joseph, A. A., Merboldt, K.-D., Ludwig, H.-C., Gärtner, J. and Frahm, J. (2015). Inspiration is the major regulator of human CSF flow. *J. Neurosci.* **35**, 2485-2491. doi:10.1523/JNEUROSCI.3246-14.2015

Driessen, R. C. H., Stassen, O. M. J. A., Sjöqvist, M., Suarez Rodriguez, F., Grolleman, J., Bouten, C. V. C. and Sahlgren, C. M. (2018). Shear stress induces expression, intracellular reorganization and enhanced Notch activation potential of Jagged1. *Integr. Biol.* **10**, 719-726. doi:10.1039/C8IB00036K

Duchemin, A.-L., Vignes, H. and Vermot, J. (2019). Mechanically activated Piezo channels modulate outflow tract valve development through the yap1 and KLF2-notch signaling axis. *eLife* **8**, e44706. doi:10.7554/eLife.44706

Dupont, S., Morsut, L., Aragona, M., Enzo, E., Giulitti, S., Cordenonsi, M., Zanconato, F., Le Digabel, J., Forcato, M., Bicciato, S. et al. (2011). Role of YAP/TAZ in mechanotransduction. *Nature* **474**, 179-183. doi:10.1038/nature10137

Eichele, G., Bodenschatz, E., Ditte, Z., Günther, A.-K., Kapoor, S., Wang, Y. and Westendorf, C. (2020). Cilia-driven flows in the brain third ventricle. *Philos. Trans. R. Soc. B Biol. Sci.* **375**, 20190154. doi:10.1098/rstb.2019.0154

Engesaeth, V. G., Warner, J. O. and Bush, A. (1993). New associations of primary ciliary dyskinesia syndrome. *Pediatr. Pulmonol.* **16**, 9-12. doi:10.1002/ppul.1950160103

Fame, R. M. and Lehtinen, M. K. (2020). Emergence and developmental roles of the cerebrospinal fluid system. *Dev. Cell* **52**, 261-275. doi:10.1016/j.devcel.2020.01.027

Fang, J. S., Coon, B. G., Gillis, N., Chen, Z., Qiu, J., Chittenden, T. W., Burt, J. M., Schwartz, M. A. and Hirschi, K. K. (2017). Shear-induced Notch-Cx37-p27 axis arrests endothelial cell cycle to enable arterial specification. *Nat. Commun.* **8**, 2149. doi:10.1038/s41467-017-01742-7

Faubel, R., Westendorf, C., Bodenschatz, E. and Eichele, G. (2016). Cilia-based flow network in the brain ventricles. *Science* **353**, 176-178. doi:10.1126/science.aae0450

Feinberg, D. A. and Mark, A. S. (1987). Human brain motion and cerebrospinal fluid circulation demonstrated with MR velocity imaging. *Radiology* **163**, 793-799. doi:10.1148/radiology.163.3.3575734

Ferreira, R. R., Vilfan, A., Jülicher, F., Supatto, W. and Vermot, J. (2017). Physical limits of flow sensing in the left-right organizer. *eLife* **6**, e25078. doi:10.7554/eLife.25078

Ferreira, R. R., Pakula, G., Klaeyle, L., Fukui, H., Vilfan, A., Supatto, W. and Vermot, J. (2018). Chiral cilia orientation in the left-right organizer. *Cell Rep.* **25**, 2008-2016; e4. doi:10.1016/j.celrep.2018.10.069

Ferreira, R. R., Fukui, H., Chow, R., Vilfan, A. and Vermot, J. (2019). The cilium as a force sensor-myth versus reality. *J. Cell Sci.* **132**, jcs213496. doi:10.1242/jcs.213496

Florian, J. A., Kosky, J. R., Ainslie, K., Pang, Z., Dull, R. O. and Tarbell, J. M. . (2003). Heparan sulfate proteoglycan is a mechanosensor on endothelial cells. *Circ. Res.* **93**, 136-142. doi:10.1161/01.RES.0000101744.47866.D5

Franco, C. A., Jones, M. L., Bernabeu, M. O., Geudens, I., Mathivet, T., Rosa, A., Lopes, F. M., Lima, A. P., Ragab, A., Collins, R. T. et al. (2015). Dynamic endothelial cell rearrangements drive developmental vessel regression. *PLoS Biol.* **13**, e1002125. doi:10.1371/journal.pbio.1002125

Gaengel, K., Genové, G., Armulik, A. and Betsholtz, C. (2009). Endothelial-mural cell signaling in vascular development and angiogenesis. *Arterioscler. Thromb. Vasc. Biol.* **29**, 630-638. doi:10.1161/ATVBAHA.107.161521

Gálvez-Santisteban, M., Chen, D., Zhang, R., Serrano, R., Nguyen, C., Zhao, L., Nerb, L., Masutani, E. M., Vermot, J., Burns, C. G. et al. (2019). Hemodynamic-mediated endocardial signaling controls in vivo myocardial reprogramming. *eLife* **8**, 1-24. doi:10.7554/eLife.44816

Gelfand, B. D., Meller, J., Pryor, A. W., Kahn, M., Bortz, P. D. S., Wamhoff, B. R. and Blackman, B. R. (2011). Hemodynamic activation of β-catenin and T-Cell-specific transcription factor signaling in vascular endothelium regulates fibronectin expression. *Arterioscler. Thromb. Vasc. Biol.* **31**, 1625-1633. doi:10.1161/ATVBAHA.111.227827

Gerhardt, H., Golding, M., Fruttiger, M., Ruhrberg, C., Lundkvist, A., Abramsson, A., Jeltsch, M., Mitchell, C., Alitalo, K., Shima, D. et al. (2003). VEGF guides angiogenic sprouting utilizing endothelial tip cell filopodia. *J. Cell Biol.* **161**, 1163-1177. doi:10.1083/jcb.200302047

Germino, G. G. (2005). Linking cilia to Wnts. *Nat. Genet.* **37**, 455-457. doi:10.1038/ng0505-455

Geudens, I., Coxam, B., Alt, S., Gebala, V., Vion, A.-C., Meier, K., Rosa, A. and Gerhardt, H. (2019). Artery-vein specification in the zebrafish trunk is pre-patterned by heterogeneous Notch activity and balanced by flow-mediated fine-tuning. *Development (Camb.)* **146**, dev181024. doi:10.1242/dev.181024

Ghaffari, S., Leask, R. L. and Jones, E. A. V. (2015). Flow dynamics control the location of sprouting and direct elongation during developmental angiogenesis. *Development (Camb.)* **142**, 4151-4157. doi:10.1242/dev.128058

Ghaffari, S., Leask, R. L. and Jones, E. A. V. (2017). Blood flow can signal during angiogenesis not only through mechanotransduction, but also by affecting growth factor distribution. *Angiogenesis* **20**, 373-384. doi:10.1007/s10456-017-9553-x

Givens, C. and Tzima, E. (2016). Endothelial mechanosignaling: does one sensor fit all? *Antioxid Redox Signal.* **25**, 373-388. doi:10.1089/ars.2015.6493

Goddard, L. M., Duchemin, A. L., Ramalingan, H., Wu, B., Chen, M., Bamezai, S., Yang, J., Li, L., Morley, M. P., Wang, T. et al. (2017). Hemodynamic forces sculpt developing heart valves through a KLF2-WNT9B paracrine signaling axis. *Dev. Cell* **43**, 274-289; e5. doi:10.1016/j.devcel.2017.09.023

Goedicke-Fritz, S., Kaistha, A., Kacik, M., Markert, S., Hofmeister, A., Busch, C., Bänfer, S., Jacob, R., Grgic, I. and Hoyer, J. (2015). Evidence for functional and dynamic microcompartmentation of Cav-1/TRPV4/K(Ca) in caveolae of endothelial cells. *Eur. J. Cell Biol.* **94**, 391-400. doi:10.1016/j.ejcb.2015.06.002

Goetz, J. G., Steed, E., Ferreira, R. R., Roth, S., Ramspacher, C., Boselli, F., Charvin, G., Liebling, M., Wyart, C., Schwab, Y. et al. (2014). Endothelial cilia mediate low flow sensing during zebrafish vascular development. *Cell Reports* **6**, 799-808. doi:10.1016/j.celrep.2014.01.032

Gortazar, A. R., Martin-Millan, M., Bravo, B., Plotkin, L. I. and Bellido, T. (2013). Crosstalk between caveolin-1/extracellular signal-regulated kinase (ERK) and β-catenin survival pathways in osteocyte mechanotransduction. *J. Biol. Chem.* **288**, 8168-8175. doi:10.1074/jbc.M112.437921

Grimes, D. T., Boswell, C. W., Morante, N. F. C., Henkelman, R. M., Burdine, R. D. and Ciruna, B. (2016). Zebrafish models of idiopathic scoliosis link cerebrospinal fluid flow defects to spine curvature. *Science* **352**, 1341-1344. doi:10.1126/science.aaf6419

Gros, J., Feistel, K., Viebahn, C., Blum, M. and Tabin, C. J. (2009). Cell movements at Hensen's node establish left/right asymmetric gene expression in the chick. *Science* **324**, 941-944. doi:10.1126/science.1172478

Guirao, B., Meunier, A., Mortaud, S., Aguilar, A., Corsi, J. M., Strehl, L., Hirota, Y., Desoeuvre, A., Boutin, C., Han, Y. G. et al. (2010). Coupling between hydrodynamic forces and planar cell polarity orients mammalian motile cilia. *Nat. Cell Biol.* **12**, 341-350. doi:10.1038/ncb2040

Hartmannsgruber, V., Heyken, W.-T., Kacik, M., Kaistha, A., Grgic, I., Harteneck, C., Liedtke, W., Hoyer, J. and Köhler, R. (2007). Arterial response to shear stress critically depends on endothelial TRPV4 expression. *PLoS ONE* **2**, e827. doi:10.1371/journal.pone.0000827

He, C., Hu, H., Braren, R., Fong, S. Y., Trumpp, A., Carlson, T. R. and Wang, R. A. (2008). C-Myc in the hematopoietic lineage is crucial for its angiogenic function in the mouse embryo. *Development* **135**, 2467-2477. doi:10.1242/dev.020131

Heckel, E., Boselli, F., Roth, S., Krudewig, A., Belting, H. G., Charvin, G. and Vermot, J. (2015). Oscillatory flow modulates mechanosensitive klf2a expression through trpv4 and trpp2 during heart valve development. *Curr. Biol.* **25**, 1354-1361. doi:10.1016/j.cub.2015.03.038

Heer, N. C. and Martin, A. C. (2017). Tension, contraction and tissue morphogenesis. *Development (Camb.)* **144**, 4249-4260. doi:10.1242/dev.151282

Henderson-Toth, C. E., Jahnsen, E. D., Jamarani, R., Al-Roubaie, S. and Jones, E. A. V. (2012). The glycocalyx is present as soon as blood flow is initiated and is required for normal vascular development. *Dev. Biol.* **369**, 330-339. doi:10.1016/j.ydbio.2012.07.009

Hierck, B. P., Van Der Heiden, K., Alkemade, F. E., Van De Pas, S., Van Thienen, J. V., Groenendijk, B. C. W., Bax, W. H., Van Der Laarse, A., DeRuiter, M. C., Horrevoets, A. J. G. et al. (2008). Primary cilia sensitize endothelial cells for fluid shear stress. *Dev. Dyn.* **237**, 725-735. doi:10.1002/dvdy.21472

Hoger, J. H., Ilyin, V. I., Forsyth, S. and Hoger, A. (2002). Shear stress regulates the endothelial Kir2.1 ion channel. *Proc. Natl. Acad. Sci. USA* **99**, 7780-7785. doi:10.1073/pnas.102184999

Hong, C. C., Peterson, Q. P., Hong, J. Y. and Peterson, R. T. (2006). Artery/vein specification is governed by opposing phosphatidylinositol-3 kinase and MAP kinase/ERK signaling. *Curr. Biol.* **16**, 1366-1372. doi:10.1016/j.cub.2006.05.046

Hove, J. R., Köster, R. W., Forouhar, A. S., Acevedo-Bolton, G., Fraser, S. E. and Gharib, M. (2003). Intracardiac fluid forces are an essential epigenetic factor for embryonic cardiogenesis. *Nature* **421**, 172-177. doi:10.1038/nature01282

Hu, N., Christensen, D. A., Agrawal, A. K., Beaumont, C., Clark, E. B. and Hawkins, J. A. (2009). Dependence of aortic arch morphogenesis on intracardiac blood flow in the left atrial ligated chick embryo. *Anat. Rec.* **292**, 652-660. doi:10.1002/ar.20885

Ibañez-Tallon, I. (2002). Loss of function of axonemal dynein Mdnah5 causes primary ciliary dyskinesia and hydrocephalus. *Hum. Mol. Genet.* **11**, 715-721. doi:10.1093/hmg/11.6.715
Ibañez-Tallon, I., Pagenstecher, A., Fliegauf, M., Olbrich, H., Kispert, A., Ketelsen, U. P., North, A., Heintz, N. and Omran, H. (2004). Dysfunction of axonemal dynein heavy chain Mdnah5 inhibits ependymal flow and reveals a novel mechanism for hydrocephalus formation. *Hum. Mol. Genet.* **13**, 2133-2141. doi:10.1093/hmg/ddh219
Jahnsen, E. D., Trindade, A., Zaun, H. C. and Lehoux, S. (2015). Notch1 Is pan-endothelial at the onset of flow and regulated by flow. *PLoS ONE* **10**, e0122622. doi:10.1371/journal.pone.0122622
Jalali, S., del Pozo, M. A., Chen, K.-D., Miao, H., Li, Y.-S., Schwartz, M. A., Shyy, J. Y.-J. and Chien, S. (2001). Integrin-mediated mechanotransduction requires its dynamic interaction with specific extracellular matrix (ECM) ligands. *Proc. Natl. Acad. Sci. USA* **98**, 1042-1046. doi:10.1073/pnas.98.3.1042
Jones, E. A. V. (2011). Mechanical factors in the development of the vascular bed. *Respir. Physiol. Neurobiol.* **178**, 59-65. doi:10.1016/j.resp.2011.03.026
Jones, E. A. V., le Noble, F. and Eichmann, A. (2006). What determines blood vessel structure? Genetic prespecification vs. hemodynamics. *Physiology* **21**, 388-395. doi:10.1152/physiol.00020.2006
Jung, B., Obinata, H., Galvani, S., Mendelson, K., Ding, B., Skoura, A., Kinzel, B., Brinkmann, V., Rafii, S., Evans, T. et al. (2012). Flow-regulated endothelial S1P receptor-1 signaling sustains vascular development. *Dev. Cell.* **23**, 600-610. doi:10.1016/j.devcel.2012.07.015
Kaiser, K., Gyllborg, D., Procházka, J., Salašová, A., Kompaníková, P., Molina, F. L., Laguna-Goya, R., Radaszkiewicz, T., Harnoš, J., Procházková, M. et al. (2019). WNT5A is transported via lipoprotein particles in the cerebrospinal fluid to regulate hindbrain morphogenesis. *Nat. Commun.* **10**, 1498. doi:10.1038/s41467-019-09298-4
Karthik, S., Djukic, T., Kim, J.-D., Zuber, B., Makanya, A., Odriozola, A., Hlushchuk, R., Filipovic, N., Jin, S. W. and Djonov, V. (2018). Synergistic interaction of sprouting and intussusceptive angiogenesis during zebrafish caudal vein plexus development. *Sci. Rep.* **8**, 9840. doi:10.1038/s41598-018-27791-6
Kasaai, B., Caolo, V., Peacock, H. M., Lehoux, S., Gomez-Perdiguero, E., Luttun, A. and Jones, E. A. V. (2017). Erythro-myeloid progenitors can differentiate from endothelial cells and modulate embryonic vascular remodeling. *Sci. Rep.* **7**, 43817. doi:10.1038/srep43817
Kazenwadel, J., Secker, G. A., Liu, Y. J., Rosenfeld, J. A., Wildin, R. S., Cuellar-Rodriguez, J., Hsu, A. P., Dyack, S., Fernandez, C. V., Chong, C. E. et al. (2012). Loss-of-function germline GATA2 mutations in patients with MDS/AML or MonoMAC syndrome and primary lymphedema reveal a key role for GATA2 in the lymphatic vasculature. *Blood* **119**, 1283-1291. doi:10.1182/blood-2011-08-374363
Kim, S., Chung, M., Ahn, J., Lee, S. and Jeon, N. L. (2016). Interstitial flow regulates the angiogenic response and phenotype of endothelial cells in a 3D culture model. *Lab. Chip* **16**, 4189-4199. doi:10.1039/C6LC00910G
Kim, J. J., Kim, Y. H., Kim, J. J., Park, D. Y., Bae, H., Lee, D.-H. H., Kim, K. H., Hong, S. P., Jang, S. P., Kubota, Y. et al. (2017). YAP/TAZ regulates sprouting angiogenesis and vascular barrier maturation. *J. Clin. Investig.* **127**, 3441-3461. doi:10.1172/JCI93825
Kim, I., Kim, J. H., Kim, K., Seong, S. and Kim, N. (2019). The IRF2BP2-KLF2 axis regulates osteoclast and osteoblast differentiation. *BMB Rep.* **52**, 469-474. doi:10.5483/BMBRep.2019.52.7.104
Kochhan, E., Lenard, A., Ellertsdottir, E., Herwig, L., Affolter, M., Belting, H. G. and Siekmann, A. F. (2013). Blood flow changes coincide with cellular rearrangements during blood vessel pruning in zebrafish embryos. *PLoS ONE* **8**, e75060. doi:10.1371/journal.pone.0075060
Konjikusic, M. J., Yeetong, P., Boswell, C. W., Lee, C., Roberson, E. C., Ittiwut, R., Suphapeetiporn, K., Ciruna, B., Gurnett, C. A., Wallingford, J. B. et al. (2018). Mutations in Kinesin family member 6 reveal specific role in ependymal cell ciliogenesis and human neurological development. *PLoS Genet.* **14**, e1007817. doi:10.1371/journal.pgen.1007817
Korn, C. and Augustin, H. G. (2015). Mechanisms of vessel pruning and regression. *Dev. Cell* **34**, 5-17. doi:10.1016/j.devcel.2015.06.004
Koushik, S. V., Wang, J., Rogers, R., Moskophidis, D., Lambert, N. A., Creazzo, T. L. and Conway, S. J. (2001). Targeted inactivation of the sodium-calcium exchanger (Ncx1) results in the lack of a heartbeat and abnormal myofibrillar organization. *FASEB J.* **15**, 1209-1211. doi:10.1096/fj.00-0696fje
Kowalski, W. J., Teslovich, N. C., Dur, O., Keller, B. B. and Pekkan, K. (2012). Computational hemodynamic optimization predicts dominant aortic arch selection is driven by embryonic outflow tract orientation in the chick embryo. *Biomech. Model. Mechanobiol.* **11**, 1057-1073. doi:10.1007/s10237-012-0373-z
Kramer-Zucker, A. G., Olale, F., Haycraft, C. J., Yoder, B. K., Schier, A. F. and Drummond, I. A. (2005). Cilia-driven fluid flow in the zebrafish pronephros, brain and Kupffer's vesicle is required for normal organogenesis. *Development* **132**, 1907-1921. doi:10.1242/dev.01772
Kuo, C. T., Veselits, M. L., Barton, K. P., Lu, M. M., Clendenin, C. and Leiden, J. M. (1997). The LKLF transcription factor is required for normal tunica media formation and blood vessel stabilization during murine embryogenesis. *Genes Dev.* **11**, 2996-3006. doi:10.1101/gad.11.22.2996
Lam, E. Y. N., Hall, C. J., Crosier, P. S., Crosier, K. E. and Flores, M. V. (2010). Live imaging of Runx1 expression in the dorsal aorta tracks the emergence of blood progenitors from endothelial cells. *Blood* **116**, 909-914. doi:10.1182/blood-2010-01-264382
Lawson, N. D., Scheer, N., Pham, V. N., Kim, C. H., Chitnis, A. B., Campos-Ortega, J. A. and Weinstein, B. M. (2001). Notch signaling is required for arterial-venous differentiation during embryonic vascular development. *Development* **128**, 3675-3683.
le Noble, F., Moyon, D., Pardanaud, L., Yuan, L., Djonov, V., Matthijsen, R., Bréant, C., Fleury, V. and Eichmann, A. (2003). Flow regulates arterial-venous differentiation in the chick embryo yolk sac. *Development* **131**, 361-375. doi:10.1242/dev.00929
Lee, L. (2013). Riding the wave of ependymal cilia: Genetic susceptibility to hydrocephalus in primary ciliary dyskinesia: ependymal cilia and PCD. *J. Neurosci. Res.* **91**, 1117-1132. doi:10.1002/jnr.23238
Levin, M., Johnson, R. L., Stern, C. D., Kuehn, M. and Tabin, C. (1995). A molecular pathway determining left-right asymmetry in chick embryogenesis. *Cell* **82**, 803-814. doi:10.1016/0092-8674(95)90477-8
Li, J., Hou, B., Tumova, S., Muraki, K., Bruns, A., Ludlow, M. J., Sedo, A., Hyman, A. J., McKeown, L., Young, R. S. et al. (2014a). Piezo1 integration of vascular architecture with physiological force. *Nature* **515**, 279-282. doi:10.1038/nature13701
Li, R., Beebe, T., Jen, N., Yu, F., Takabe, W., Harrison, M., Cao, H., Lee, J., Yang, H., Han, P. et al. (2014b). Shear stress-activated Wnt-angiopoietin-2 signaling recapitulates vascular repair in zebrafish embryos. *Arterioscler. Thromb. Vasc. Biol.* **34**, 2268-2275. doi:10.1161/ATVBAHA.114.303345
Liew, H., Roberts, M. A., MacGinley, R. and McMahon, L. P. (2017). Endothelial glycocalyx in health and kidney disease: rising star or false Dawn? *Nephrology* **22**, 940-946. doi:10.1111/nep.13161
Lim, K. C., Hosoya, T., Brandt, W., Ku, C. J., Hosoya-Ohmura, S., Camper, S. A., Yamamoto, M. and Engel, J. D. (2012). Conditional Gata2 inactivation results in HSC loss and lymphatic mispatterning. *J. Clin. Investig.* **122**, 3705-3717. doi:10.1172/JCI61619
Lin, Y. F., Swinburne, I. and Yelon, D. (2012). Multiple influences of blood flow on cardiomyocyte hypertrophy in the embryonic zebrafish heart. *Dev. Biol.* **362**, 242-253. doi:10.1016/j.ydbio.2011.12.005
Logan, M., Pagán-Westphal, S. M., Smith, D. M., Paganessi, L. and Tabin, C. J. (1998). The transcription factor Pitx2 mediates situs-specific morphogenesis in response to left-right asymmetric signals. *Cell* **94**, 307-317. doi:10.1016/S0092-8674(00)81474-9
Lowery, L. A. and Sive, H. (2009). Totally tubular: The mystery behind function and origin of the brain ventricular system. *BioEssays* **31**, 446-458. doi:10.1002/bies.200800207
Lucitti, J. L., Jones, E. A. V., Huang, C., Chen, J., Fraser, S. E. and Dickinson, M. E. (2007). Vascular remodeling of the mouse yolk sac requires hemodynamic force. *Development* **134**, 3317-3326. doi:10.1242/dev.02883
Lundin, V., Sugden, W. W., Theodore, L. N., Sousa, P. M., Han, A., Chou, S., Wrighton, P. J., Cox, A. G., Ingber, D. E., Goessling, W. et al. (2020). YAP regulates hematopoietic stem cell formation in response to the biomechanical forces of blood flow. *Dev. Cell* **52**, 446-460. doi:10.1016/j.devcel.2020.01.006
Ma, X., Qiu, S., Luo, J., Ma, Y., Ngai, C. Y., Shen, B., Wong, C. O., Huang, Y. and Yao, X. (2010). Functional role of vanilloid transient receptor potential 4-canonical transient receptor potential 1 complex in flow-induced ca^{2+} influx. *Arterioscler. Thromb. Vasc. Biol.* **30**, 851-858. doi:10.1161/ATVBAHA.109.196584
Mack, J. J., Mosqueiro, T. S., Archer, B. J., Jones, W. M., Sunshine, H., Faas, G. C., Briot, A., Aragón, R. L., Su, T., Romay, M. C. et al. (2017). NOTCH1 is a mechanosensor in adult arteries. *Nat. Commun.* **8**, 1-18. doi:10.1038/s41467-017-01741-8
Masuyama, R., Vriens, J., Voets, T., Karashima, Y., Owsianik, G., Vennekens, R., Lieben, L., Torrekens, S., Moermans, K., Vanden Bosch, A. et al. (2008). TRPV4-mediated calcium influx regulates terminal differentiation of osteoclasts. *Cell Metab.* **8**, 257-265. doi:10.1016/j.cmet.2008.08.002
McGirt, M. J., Atiba, A., Attenello, F. J., Wasserman, B. A., Datoo, G., Gathinji, M., Carson, B., Weingart, J. D. and Jallo, G. I. (2008). Correlation of hindbrain CSF flow and outcome after surgical decompression for Chiari I malformation. *Child's Nervous Syst.* **24**, 833-840. doi:10.1007/s00381-007-0569-1
McGrath, K. E., Koniski, A. D., Malik, J. and Palis, J. (2003). Circulation is established in a stepwise pattern in the mammalian embryo. *Blood* **101**, 1669-1675. doi:10.1182/blood-2002-08-2531
Medvinsky, A. and Dzierzak, E. (1996). Definitive hematopoiesis is autonomously initiated by the AGM region. *Cell* **86**, 897-906. doi:10.1016/S0092-8674(00)80165-8
Mehta, V., Pang, K. L., Rozbesky, D., Nather, K., Keen, A., Lachowski, D., Kong, Y., Karia, D., Ameismeier, M., Huang, J. et al. (2020). The guidance receptor plexin D1 is a mechanosensor in endothelial cells. *Nature* **578**, 290-295. doi:10.1038/s41586-020-1979-4
Melchior, B. and Frangos, J. A. (2010). Shear-induced endothelial cell-cell junction inclination. *Am. J. Physiol. Cell Physiol.* **299**, C621. doi:10.1152/ajpcell.00156.2010

Minegishi, K., Hashimoto, M., Ajima, R., Takaoka, K., Shinohara, K., Ikawa, Y., Nishimura, H., McMahon, A. P., Willert, K., Okada, Y. et al. (2017). A Wnt5 activity asymmetry and intercellular signaling via PCP proteins polarize node cells for left-right symmetry breaking. *Dev. Cell* **40**, 439-452.e4. doi:10.1016/j.devcel.2017.02.010

Mirzadeh, Z., Han, Y.-G., Soriano-Navarro, M., García-Verdugo, J. M. and Alvarez-Buylla, A. (2010). Cilia organize ependymal planar polarity. *J. Neurosci.* **30**, 2600-2610. doi:10.1523/JNEUROSCI.3744-09.2010

Mitchell, B., Jacobs, R., Li, J., Chien, S. and Kintner, C. (2007). A positive feedback mechanism governs the polarity and motion of motile cilia. *Nature* **447**, 97-101. doi:10.1038/nature05771

Moyon, D., Pardanaud, L., Yuan, L., Bréant, C. and Eichmann, A. (2001). Plasticity of endothelial cells during arterial-venous differentiation in the avian embryo. *Development* **128**, 3359-3370.

Müller, A. M., Medvinsky, A., Strouboulis, J., Grosveld, F. and Dzierzakt, E. (1994). Development of hematopoietic stem cell activity in the mouse embryo. *Immunity* **1**, 291-301. doi:10.1016/1074-7613(94)90081-7

Nakajima, H., Yamamoto, K., Agarwala, S., Terai, K., Fukui, H., Fukuhara, S., Ando, K., Miyazaki, T., Yokota, Y., Schmelzer, E. et al. (2017). Flow-dependent endothelial YAP regulation contributes to vessel maintenance. *Dev. Cell* **40**, 523-536.e6. doi:10.1016/j.devcel.2017.02.019

Nauli, S. M., Alenghat, F. J., Luo, Y., Williams, E., Vassilev, P., Li, X., Elia, A. E. H., Lu, W., Brown, E. M., Quinn, S. J. et al. (2003). Polycystins 1 and 2 mediate mechanosensation in the primary cilium of kidney cells. *Nat. Genet.* **33**, 129-137. doi:10.1038/ng1076

Nauli, S. M., Kawanabe, Y., Kaminski, J. J., Pearce, W. J., Ingber, D. E. and Zhou, J. (2008). Endothelial cilia are fluid shear sensors that regulate calcium signaling and nitric oxide production through Polycystin-1. *Circulation* **117**, 1161-1171. doi:10.1161/CIRCULATIONAHA.107.710111

Nishii, K. and Shibata, Y. (2006). Mode and determination of the initial contraction stage in the mouse embryo heart. *Anat. Embryol.* **211**, 95-100. doi:10.1007/s00429-005-0065-x

Nonaka, S., Tanaka, Y., Okada, Y., Takeda, S., Harada, A., Kanai, Y., Kido, M. and Hirokawa, N. (1998). Randomization of left-right asymmetry due to loss of nodal cilia generating leftward flow of extraembryonic fluid in mice lacking KIF3B motor protein. *Cell* **95**, 829-837. doi:10.1016/S0092-8674(00)81705-5

Nonaka, S., Shiratori, H., Saijoh, Y. and Hamada, H. (2002). Determination of left-right patterning of the mouse embryo by artificial nodal flow. *Nature* **418**, 96-99. doi:10.1038/nature00849

Nonaka, S., Yoshiba, S., Watanabe, D., Ikeuchi, S., Goto, T., Marshall, W. F. and Hamada, H. (2005). De novo formation of left–right asymmetry by posterior tilt of nodal cilia. *PLoS Biol.* **3**, e268. doi:10.1371/journal.pbio.0030268

Nonomura, K., Lukacs, V., Sweet, D. T., Goddard, L. M., Kanie, A., Whitwam, T., Ranade, S. S., Fujimori, T., Kahn, M. L. and Patapoutian, A. (2018). Mechanically activated ion channel PIEZO1 is required for lymphatic valve formation. *Proc. Natl Acad. Sci. USA* **115**, 12817-12822. doi:10.1073/pnas.1817070115

North, T. E., Goessling, W., Peeters, M., Li, P., Ceol, C., Lord, A. M., Weber, G. J., Harris, J., Cutting, C. C., Huang, P. et al. (2009). Hematopoietic stem cell development is dependent on blood flow. *NIH Public Access* **137**, 736-748. doi:10.1016/j.cell.2009.04.023

Ohata, S., Herranz-Pérez, V., Nakatani, J., Boletta, A., García-Verdugo, J. M. and Álvarez-Buylla, A. (2015). Mechanosensory genes Pkd1 and Pkd2 contribute to the planar polarization of brain ventricular epithelium. *J. Neurosci.* **35**, 11153-11168. doi:10.1523/JNEUROSCI.0686-15.2015

Ohata, S., Álvarez-Buylla, A. and Alvarez-Buylla, A. (2016). Planar organization of multiciliated ependymal (E1) cells in the brain ventricular epithelium. *Trends Neurosci.* **39**, 543-551. doi:10.1016/j.tins.2016.05.004

Okabe, N., Xu, B. and Burdine, R. D. (2008). Fluid dynamics in zebrafish Kupffer's vesicle. *Dev. Dyn.* **237**, 3602-3612. doi:10.1002/dvdy.21730

Okada, Y., Takeda, S., Tanaka, Y., Belmonte, J. C. I. and Hirokawa, N. (2005). Mechanism of nodal flow: A conserved symmetry breaking event in left-right axis determination. *Cell* **121**, 633-644. doi:10.1016/j.cell.2005.04.008

Olesen, S.-P., Claphamt, D. and Davies, P. (1988). Haemodynamic shear stress activates a K^+ current in vascular endothelial cells. *Nature* **331**, 168-170. doi:10.1038/331168a0

Olstad, E. W., Ringers, C., Hansen, J. N., Wens, A., Brandt, C., Wachten, D., Yaksi, E. and Jurisch-Yaksi, N. (2019). Ciliary beating compartmentalizes cerebrospinal fluid flow in the brain and regulates ventricular development. *Curr. Biol.* **29**, 229-241; e6. doi:10.1016/j.cub.2018.11.059

Omori, T., Winter, K., Shinohara, K., Hamada, H. and Ishikawa, T. (2018). Simulation of the nodal flow of mutant embryos with a small number of cilia: comparison of mechanosensing and vesicle transport hypotheses. *R. Soc. Open Sci.* **5**, 1-15. doi:10.1098/rsos.180601

Outeda, P., Huso, D. L., Fisher, S. A., Halushka, M. K., Kim, H., Qian, F., Germino, G. G. and Watnick, T. (2014). Polycystin signaling is required for directed endothelial cell migration and lymphatic development. *Cell Rep.* **7**, 634-644. doi:10.1016/j.celrep.2014.03.064

Panigrahi, M., Reddy, B. P., Reddy, A. K. and Reddy, J. J. M. (2004). CSF flow study in Chiari I malformation. *Child's Nervous Syst.* **20**, 336-340. doi:10.1007/s00381-003-0881-3

Parmar, K. M., Larman, H. B., Dai, G., Zhang, Y., Wang, E. T., Moorthy, S. N., Kratz, J. R., Lin, Z., Jain, M. K., Jr, M. A. G. and García-cardeña, G. (2006). Integration of flow-dependent endothelial phenotypes by Kruppel-like factor 2. *J. Clin. Invest.* **116**, 49-58. doi:10.1172/JCI24787

Peacock, H. M., Tabibian, A., Criem, N., Caolo, V., Hamard, L., Deryckere, A., Haefliger, J.-A., Kwak, B. R., Zwijsen, A. and Jones, E. A. V. (2020). Impaired SMAD1/5 Mechanotransduction and Cx37 (Connexin37) expression enable pathological vessel enlargement and shunting. *Arterioscler. Thromb. Vasc. Biol.* **40**, e87-e104. doi:10.1161/ATVBAHA.119.313122

Peshkovsky, C., Totong, R. and Yelon, D. (2011). Dependence of cardiac trabeculation on neuregulin signaling and blood flow in zebrafish. *Dev. Dyn.* **240**, 446-456. doi:10.1002/dvdy.22526

Petrova, T. V., Karpanen, T., Norrmén, C., Mellor, R., Tamakoshi, T., Finegold, D., Ferrell, R., Kerjaschki, D., Mortimer, P., Ylä-Herttuala, S. et al. (2004). Defective valves and abnormal mural cell recruitment underlie lymphatic vascular failure in lymphedema distichiasis. *Nat. Med.* **10**, 974-981. doi:10.1038/nm1094

Peyronnet, R., Martins, J. R., Duprat, F., Demolombe, S., Arhatte, M., Jodar, M., Tauc, M., Duranton, C., Paulais, M., Teulon, J. et al. (2013). Piezo1-dependent stretch-activated channels are inhibited by Polycystin-2 in renal tubular epithelial cells. *EMBO Rep.* **14**, 1143-1148. doi:10.1038/embor.2013.170

Piccolo, S., Agius, E., Leyns, L., Bhattacharyya, S., Grunz, H., Bouwmeester, T. and De Robertis, E. M. (1999). The head inducer cerberus is a multifunctional antagonist of Nodal, BMP and Wnt signals. *Nature* **397**, 707-710. doi:10.1038/17820

Pochynyuk, O., Zaika, O., O'Neil, R. G. and Mamenko, M. (2013). Novel insights into TRPV4 function in the kidney. *Pflugers Arch. Eur. J. Physiol.* **465**, 177-186. doi:10.1007/s00424-012-1190-z

Praetorius, H. A. and Spring, K. R. (2003). The renal cell primary cilium functions as a flow sensor. *Curr. Opin Nephrol. Hypertens.* **12**, 517-520. doi:10.1097/00041552-200309000-00006

Ranade, S. S., Qiu, Z., Woo, S., Sik, S. and Murthy, S. E. (2014). Piezo1, a mechanically activated ion channel, is required for vascular development in mice. *Proc. Natl. Acad. Sci. USA* **111**, 10347-10352. doi:10.1073/pnas.1409233111

Rasouli, S. J., El-Brolosy, M., Tsedeke, A. T., Bensimon-Brito, A., Ghanbari, P., Maischein, H.-M., Kuenne, C. and Stainier, D. Y. (2018). The flow responsive transcription factor Klf2 is required for myocardial wall integrity by modulating Fgf signaling. *eLife* **7**, 1-27. doi:10.7554/eLife.38889

Ricard, N., Ciais, D., Levet, S., Subileau, M., Mallet, C., Zimmers, T. A., Lee, S. J., Bidart, M., Feige, J. J. and Bailly, S. (2012). BMP9 and BMP10 are critical for postnatal retinal vascular remodeling. *Blood* **119**, 6162-6171. doi:10.1182/blood-2012-01-407593

Ringers, C., Olstad, E. W. and Jurisch-Yaksi, N. (2020). The role of motile cilia in the development and physiology of the nervous system. *Philos. Trans. R. Soc. B Biol. Sci.* **375**, 1-11. doi:10.1098/rstb.2019.0156

Rizzo, V., Morton, C., DePaola, N., Schnitzer, J. E. and Davies, P. F. (2003). Recruitment of endothelial caveolae into mechanotransduction pathways by flow conditioning in vitro. *Am. J. Physiol. Heart Circ. Physiol.* **285**, H1720-H1729. doi:10.1152/ajpheart.00344.2002

Ryan, A. K., Blumberg, B., Rodriguez-Esteban, C., Yonei-Tamura, S., Tamura, K., Tsukui, T., de la Peña, J., Sabbagh, W., Greenwald, J., Choe, S. et al. (1998). Pitx2 determines left-right asymmetry of internal organs in vertebrates. *Nature* **394**, 545-551. doi:10.1038/29004

Sabine, A., Agalarov, Y., Maby-El Hajjami, H., Jaquet, M., Hägerling, R., Pollmann, C., Bebber, D., Pfenniger, A., Miura, N., Dormond, O. et al. (2012). Mechanotransduction, PROX1, and FOXC2 cooperate to control Connexin37 and calcineurin during lymphatic-valve formation. *Dev. Cell* **22**, 430-445. doi:10.1016/j.devcel.2011.12.020

Sabine, A., Bovay, E., Demir, C. S., Kimura, W., Jaquet, M., Agalarov, Y., Zangger, N., Scallan, J. P., Graber, W., Gulpinar, E. et al. (2015). FOXC2 and fluid shear stress stabilize postnatal lymphatic vasculature. *J. Clin. Investig.* **125**, 3861-3877. doi:10.1172/JCI80454

Samokhvalov, I. M., Samokhvalova, N. I. and Nishikawa, S. (2007). Cell tracing shows the contribution of the yolk sac to adult haematopoiesis. *Nature* **446**, 1056-1061. doi:10.1038/nature05725

Sampaio, P., Ferreira, R. R., Guerrero, A., Pintado, P., Tavares, B., Amaro, J., Smith, A. A., Montenegro-Johnson, T., Smith, D. J. and Lopes, S. S. (2014). Left-right organizer flow dynamics: How much cilia activity reliably yields laterality? *Dev. Cell* **29**, 716-728. doi:10.1016/j.devcel.2014.04.030

Samsa, L. A., Givens, C., Tzima, E., Stainier, D. Y. R., Qian, L. and Liu, J. (2015). Cardiac contraction activates endocardial notch signaling to modulate chamber maturation in zebrafish. *Development (Camb.)* **142**, 4080-4091. doi:10.1242/dev.125724

Satyanarayana, A., Gudmundsson, K. O., Chen, X., Coppola, V., Tessarollo, L., Keller, J. R. and Hou, S. X. (2010). RapGEF2 is essential for embryonic hematopoiesis but dispensable for adult hematopoiesis. *Blood* **116**, 2921-2931. doi:10.1182/blood-2010-01-262964

Sawamoto, K., Wichterle, H., Gonzalez-Perez, O., Cholfin, J. A., Yamada, M., Spassky, N., Murcia, N. S., Garcia-Verdugo, J. M., Marin, O., Rubenstein, J. L. R. et al. (2006). New neurons follow the flow of cerebrospinal fluid in the adult brain. *Science* **311**, 629-632. doi:10.1126/science.1119133

Schottenfeld, J., Sullivan-Brown, J. and Burdine, R. D. (2007). Zebrafish curly up encodes a Pkd2 ortholog that restricts left-side-specific expression of southpaw. *Development* **134**, 1605-1615. doi:10.1242/dev.02827

Sehnert, A. J., Huq, A., Weinstein, B. M., Walker, C., Fishman, M. and Stainier, D. Y. R. (2002). Cardiac troponin T is essential in sarcomere assembly and cardiac contractility. *Nat. Genet.* **31**, 106-110. doi:10.1038/ng875

Sinha, B., Köster, D., Ruez, R., Gonnord, P., Bastiani, M., Abankwa, D., Stan, R. V., Butler-Browne, G., Vedie, B., Johannes, L. et al. (2011). Cells respond to mechanical stress by rapid disassembly of caveolae. *Cell* **144**, 402-413. doi:10.1016/j.cell.2010.12.031

Siyahhan, B., Knobloch, V., de Zélicourt, D., Asgari, M., Schmid Daners, M., Poulikakos, D. and Kurtcuoglu, V. (2014). Flow induced by ependymal cilia dominates near-wall cerebrospinal fluid dynamics in the lateral ventricles. *J. R. Soc. Interface* **11**, 20131189. doi:10.1098/rsif.2013.1189

Slough, J., Cooney, L. and Brueckner, M. (2008). Monocilia in the embryonic mouse heart suggest a direct role for cilia in cardiac morphogenesis. *Dev. Dyn.* **237**, 2304-2314. doi:10.1002/dvdy.21669

Song, J. W. and Munn, L. L. (2011). Fluid forces control endothelial sprouting. *Proc. Natl. Acad. Sci. USA* **108**, 15342-15347. doi:10.1073/pnas.1105316108

Song, H., Hu, J., Chen, W., Elliott, G., Andre, P., Gao, B. and Yang, Y. (2010). Planar cell polarity breaks bilateral symmetry by controlling ciliary positioning. *Nature* **466**, 378-382. doi:10.1038/nature09129

Souilhol, C., Serbanovic-Canic, J., Fragiadaki, M., Chico, T. J., Ridger, V., Roddie, H. and Evans, P. C. (2019). Endothelial responses to shear stress in atherosclerosis: a novel role for developmental genes. *Nat. Rev. Cardiol.* **17**, 52-63. doi:10.1038/s41569-019-0239-5

Spassky, N., Merkle, F. T., Flames, N., Tramontin, A. D., García-Verdugo, J. M. and Alvarez-Buylla, A. (2005). Adult ependymal cells are postmitotic and are derived from radial glial cells during embryogenesis. *J. Neurosci.* **25**, 10-18. doi:10.1523/JNEUROSCI.1108-04.2005

Steed, E., Faggianelli, N., Roth, S., Ramspacher, C., Concordet, J.-P. and Vermot, J. (2016). Klf2a couples mechanotransduction and zebrafish valve morphogenesis through fibronectin synthesis. *Nat. Commun.* **7**, 11646. doi:10.1038/ncomms11646

Sternberg, J. R., Prendergast, A. E., Brosse, L., Cantaut-Belarif, Y., Thouvenin, O., Orts-Del'Immagine, A., Castillo, L., Djenoune, L., Kurisu, S., McDearmid, J. R. et al. (2018). Pkd2l1 is required for mechanoception in cerebrospinal fluid-contacting neurons and maintenance of spine curvature. *Nat. Commun.* **9**, 1-10. doi:10.1038/s41467-018-06225-x

Sweet, D. T., Jiménez, J. M., Chang, J., Hess, P. R., Mericko-Ishizuka, P., Fu, J., Xia, L., Davies, P. F. and Kahn, M. L. (2015). Lymph flow regulates collecting lymphatic vessel maturation in vivo. *J. Clin. Investig.* **125**, 2995-3007. doi:10.1172/JCI79386

Szeto, S. G., Narimatsu, M., Lu, M., He, X., Sidiqi, A. M., Tolosa, M. F., Chan, L., De Freitas, K., Bialik, J. F., Majumder, S. et al. (2016). YAP/TAZ are mechanoregulators of TGF-β-smad signaling and renal fibrogenesis. *J. Am. Soc. Nephrol.* **27**, 3117-3128. doi:10.1681/ASN.2015050499

Taber, L. A. (2006). Biophysical mechanisms of cardiac looping. *Int. J. Dev. Biol.* **50**, 323-332. doi:10.1387/ijdb.052045lt

Tabin, C. J. and Vogan, K. J. (2003). A two-cilia model for vertebrate left-right axis specification. *Genes Dev.* **17**, 1-6. doi:10.1101/gad.1053803

Tanaka, Y., Okada, Y. and Hirokawa, N. (2005). FGF-induced vesicular release of Sonic hedgehog and retinoic acid in leftward nodal flow is critical for left-right determination. *Nature* **435**, 172-177. doi:10.1038/nature03494

Tanaka, Y., Hayashi, M., Kubota, Y., Nagai, H., Sheng, G., Nishikawa, S. I. and Samokhvalov, I. M. (2012). Early ontogenic origin of the hematopoietic stem cell lineage. *Proc. Natl. Acad. Sci. USA* **109**, 4515-4520. doi:10.1073/pnas.1115828109

Teräväinen, T. P., Myllymäki, S. M., Friedrichs, J., Strohmeyer, N., Moyano, J. V., Wu, C., Matlin, K. S., Muller, D. J. and Manninen, A. (2013). αV-integrins are required for mechanotransduction in MDCK epithelial cells. *PLoS ONE* **8**, e71485. doi:10.1371/journal.pone.0071485

Thi, M. M., Suadicani, S. O., Schaffler, M. B., Weinbaum, S. and Spray, D. C. (2013). Mechanosensory responses of osteocytes to physiological forces occur along processes and not cell body and require αvβ3 integrin. *Proc. Natl. Acad. Sci. USA* **110**, 21012-21017. doi:10.1073/pnas.1321210110

Thouvenin, O., Keiser, L., Cantaut-Belarif, Y., Carbo-Tano, M., Verweij, F., Jurisch-Yaksi, N., Bardet, P.-L., van Niel, G., Gallaire, F. and Wyart, C. (2020). Origin and role of the cerebrospinal fluid bidirectional flow in the central canal. *eLife* **9**, e47699. doi:10.7554/eLife.47699

Tressel, S. L., Huang, R. P., Tomsen, N. and Jo, H. (2007). Laminar shear inhibits tubule formation and migration of endothelial cells by an angiopoietin-2-dependent mechanism. *Arterioscler. Thromb. Vasc. Biol.* **27**, 2150-2156. doi:10.1161/ATVBAHA.107.150920

Tzima, E., Del Pozo, M. A., Shattil, S. J., Chien, S. and Schwartz, M. A. (2001). Activation of integrins in endothelial cells by fluid shear stress mediates Rho-dependent cytoskeletal alignment. *EMBO J.* **20**, 4639-4647. doi:10.1093/emboj/20.17.4639

Tzima, E., Irani-Tehrani, M., Kiosses, W. B., Dejana, E., Schultz, D. A., Engelhardt, B., Cao, G., DeLisser, H. and Schwartz, M. A. (2005). A mechanosensory complex that mediates the endothelial cell response to fluid shear stress. *Nature* **437**, 426-431. doi:10.1038/nature03952

Udan, R. S., Vadakkan, T. J. and Dickinson, M. E. (2013). Dynamic responses of endothelial cells to changes in blood flow during vascular remodeling of the mouse yolk sac. *Development* **140**, 4041-4050. doi:10.1242/dev.096255

van de Pavert, S. A. and Mebius, R. E. (2010). New insights into the development of lymphoid tissues. *Nat. Rev. Immunol.* **10**, 664-674. doi:10.1038/nri2832

Vermot, J., Forouhar, A. S., Liebling, M., Wu, D., Plummer, D., Gharib, M. and Fraser, S. E. (2009). Reversing blood flows act through klf2a to ensure normal valvulogenesis in the developing heart. *PLoS Biol.* **7**, 1-14. doi:10.1371/journal.pbio.1000246

Vick, P., Kreis, J., Schneider, I., Tingler, M., Getwan, M., Thumberger, T., Beyer, T., Schweickert, A. and Blum, M. (2018). An early function of polycystin-2 for left-right organizer induction in xenopus. *IScience* **2**, 76-85. doi:10.1016/j.isci.2018.03.011

Wang, G., Cadwallader, A. B., Jang, D. S., Tsang, M., Yost, H. J. and Amack, J. D. (2011a). The Rho kinase rock2b establishes anteroposterior asymmetry of the ciliated Kupffer's vesicle in zebrafish. *Development* **138**, 45-54. doi:10.1242/dev.052985

Wang, L., Zhang, P., Wei, Y., Gao, Y., Patient, R. and Liu, F. (2011b). A blood flow-dependent klf2a-NO signaling cascade is required for stabilization of hematopoietic stem cell programming in zebrafish embryos. *Blood* **118**, 4102-4110. doi:10.1182/blood-2011-05-353235

Wang, L., You, X., Lotinun, S., Zhang, L., Wu, N. and Zou, W. (2020). Mechanical sensing protein PIEZO1 regulates bone homeostasis via osteoblast-osteoclast crosstalk. *Nat. Commun.* **11**, 282. doi:10.1038/s41467-019-14146-6

Weijts, B., Gutierrez, E., Saikin, S. K., Ablooglu, A. J., Traver, D., Groisman, A. and Tkachenko, E. (2018). Blood flow-induced Notch activation and endothelial migration enable vascular remodeling in zebrafish embryos. *Nat. Commun.* **9**, 5314. doi:10.1038/s41467-018-07732-7

Whitfield, J. F. (2003). Primary cilium-is it an osteocyte's strain-sensing flowmeter? *J. Cell. Biochem.* **89**, 233-237. doi:10.1002/jcb.10509

Winokurow, N. and Schumacher, S. (2019). A role for polycystin-1 and polycystin-2 in neural progenitor cell differentiation. *Cell. Mol. Life Sci.* **76**, 2851-2869. doi:10.1007/s00018-019-03072-x

Wittig, J. and Münsterberg, A. (2016). The early stages of heart development: insights from chicken embryos. *J. Cardiovas. Dev. Dis.* **3**, 12. doi:10.3390/jcdd3020012

Worthington, W. C. and Cathcart, R. S. (1966). Ciliary currents on ependymal surfaces. *Ann. N. Y. Acad. Sci.* **130**, 944-950. doi:10.1111/j.1749-6632.1966.tb12638.x

Xiao, Z., Dallas, M., Qiu, N., Nicolella, D., Cao, L., Johnson, M., Bonewald, L. and Quarles, L. D. (2011). Conditional deletion of Pkd1 in osteocytes disrupts skeletal mechanosensing in mice. *FASEB J.* **25**, 2418-2432. doi:10.1096/fj.10-180299

Xu, Q., Yu, S. B., Zheng, N., Yuan, X. Y., Chi, Y. Y., Liu, C., Wang, X. M., Lin, X. T. and Sui, H. J. (2016). Head movement, an important contributor to human cerebrospinal fluid circulation. *Sci. Rep.* **6**, 31787. doi:10.1038/srep31787

Yamamoto, K. and Ando, J. (2013). Endothelial cell and model membranes respond to shear stress by rapidly decreasing the order of their lipid phases. *J. Cell Sci.* **126**, 1227-1234. doi:10.1242/jcs.119628

Yang, H., Guan, L., Li, S., Jiang, Y., Xiong, N., Li, L., Wu, C., Zeng, H. and Liu, Y. (2016). Mechanosensitive caveolin-1 activation-induced PI3K/Akt/mTOR signaling pathway promotes breast cancer motility, invadopodia formation and metastasis in vivo. *Oncotarget* **7**, 16227-16247. doi:10.18632/oncotarget.7583

Yashiro, K., Shiratori, H. and Hamada, H. (2007). Haemodynamics determined by a genetic programme govern asymmetric development of the aortic arch. *Nature* **450**, 285-288. doi:10.1038/nature06254

Yoder, M. C., Hiatt, K., Dutt, P., Mukherjee, P., Bodine, D. M. and Orlic, D. (1997). Characterization of definitive lymphohematopoietic stem cells in the day 9 murine yolk sac. *Immunity* **7**, 335-344. doi:10.1016/S1074-7613(00)80355-6

Yokomizo, T. and Dzierzak, E. (2010). Three-dimensional cartography of hematopoietic clusters in the vasculature of whole mouse embryos. *Development* **137**, 3651-3661. doi:10.1242/dev.051094

Yoshiba, S., Shiratori, H., Kuo, I. Y., Kawasumi, A., Shinohara, K., Nonaka, S., Asai, Y., Sasaki, G., Belo, J. A., Sasaki, H. et al. (2012). Cilia at the node of mouse embryos sense fluid flow for left-right determination via Pkd2. *Science* **338**, 226-231. doi:10.1126/science.1222538

Yuan, S., Zhao, L., Brueckner, M. and Sun, Z. (2015). Intraciliary calcium oscillations initiate vertebrate left-right asymmetry. *Curr. Biol.* **25**, 556-567. doi:10.1016/j.cub.2014.12.051

Zhang, H., von Gise, A., Liu, Q., Hu, T., Tian, X., He, L., Pu, W., Huang, X., He, L., Cai, C.-L. et al. (2014). Yap1 is required for endothelial to mesenchymal transition of the atrioventricular cushion. *J. Biol. Chem.* **289**, 18681-18692. doi:10.1074/jbc.M114.554584

Zhang, X., Jia, S., Chen, Z., Chong, Y. L., Xie, H., Feng, D., Wu, X., Song, D. Z., Roy, S. and Zhao, C. (2018). Cilia-driven cerebrospinal fluid flow directs expression of urotensin neuropeptides to straighten the vertebrate body axis. *Nat. Genet.* **50**, 1666-1673. doi:10.1038/s41588-018-0260-3

Zhong, T. P., Rosenberg, M., Mohideen, M.-A. P. K., Weinstein, B. and Fishman, M. C. (2000). Gridlock, an HLH gene required for assembly of the aorta in zebrafish. *Science* **287**, 1820-1824. doi:10.1126/science.287.5459.1820

Zhong, F., Lee, K. and He, J. C. (2018). Role of Krüppel-like factor-2 in kidney disease: role of KLF2 in kidney disease. *Nephrology* **23**, 53-56. doi:10.1111/nep.13456

Zhou, J., Lee, P., Tsai, C., Lee, C., Yang, T., Chuang, H., Lin, W., Lin, T., Lim, S., Wei, S. et al. (2012). Force-specific activation of Smad1/5 regulates vascular endothelial cell cycle progression in response to disturbed flow. *Proc. Natl. Acad. Sci. U.S.A.* **109**, 7770-7775. doi:10.1073/pnas.1205476109